Inverse Problems Applied to Bolometer Diagnostics in Magnetic Fusion Experiments

Byron Peterson

National Institute for Fusion Science, SOKENDAI

Toki, Japan

with cooperation from:

D. Zhang, IPP; J. Jang, KFE; F. Federici, ORNL

13th ITER International School

December 9th, 2024

Outline

- Bolometer diagnostics
  - Bolometry and sources of radiation
  - Resistive bolometers (RB)
  - Imaging bolometers (IRVB)
- Geometry matrix calculation
- Synthetic diagnostics
  - for comparison of plasma model with experimental data
  - utilization for diagnostic design
- Tomography examples:
  - 1D using SVD with RB in LHD
  - 2D using RGS with RB in W7-X
  - 2D using Phillips Tikhonov with 1 IRVB in KSTAR
  - 3D using Tikhonov with 4 IRVBs in LHD
  - 2D using SART and Bayesian with RBs and IRVB in MAST-U
- Conclusion

Bolometry

- Measures total radiation (and neutrals) from plasma
- From IR to soft x-rays
- No wavelength (photon energy) discrimination
- Estimate radiative power loss for power balance
- Used to study role of impurities
- Upper energy limit depends on foil thickness

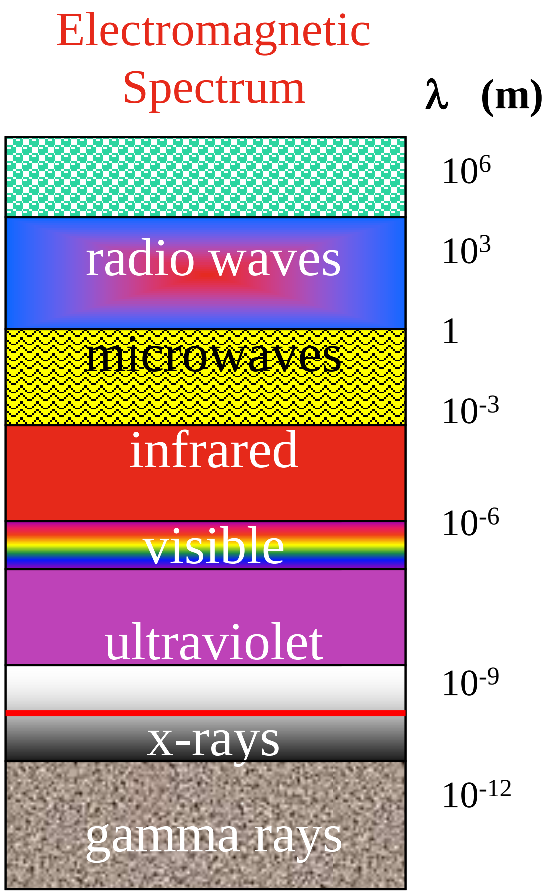

Power Balance (reactor)

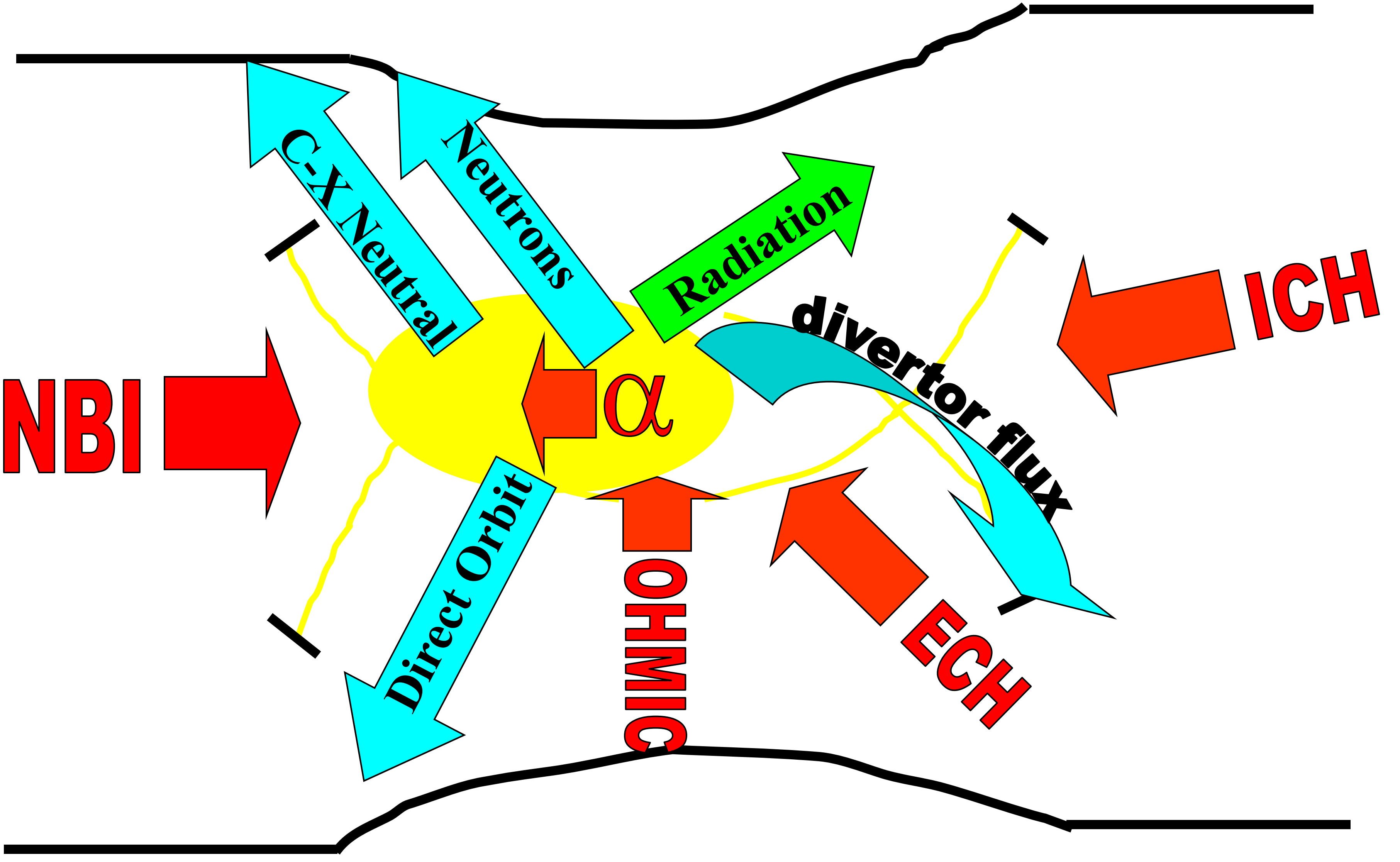

Sources of Radiation

$$(T_e = 4\,keV, n_e = 4\times10^{13}/cm^3, V = 30m^3, Z_{eff} = 3, B = 2.5T)$$

- free electron - Cyclotron (38 kW)

$$S_c = 5\times10^{-38} n_e^2 T_e^2 (W/cm^3)$$

- ion-electron interaction - Bremsstrahlung (38 kW)

$$S_{Br} = 1.7\times10^{-32} n_e T_e^{1/2} \sum_Z Z^2 n_Z = 1.7\times10^{-32} n_e^2 T_e^{1/2} Z_{eff} (W/cm^3)$$

- free-bound transition - Recombination

$$S_r = 1.7\times10^{-32} n_e T_e^{1/2} \sum_Z Z^2 n_Z \frac{E_\infty^{Z-1}}{T_e} (W/cm^3)$$

- bound electrons - Line radiation of impurities

$$S_{imp} = \sum_{n,Z} n_e n_{n,Z} L_{n,Z}(T_e)$$

Predominant source is impurity line radiation

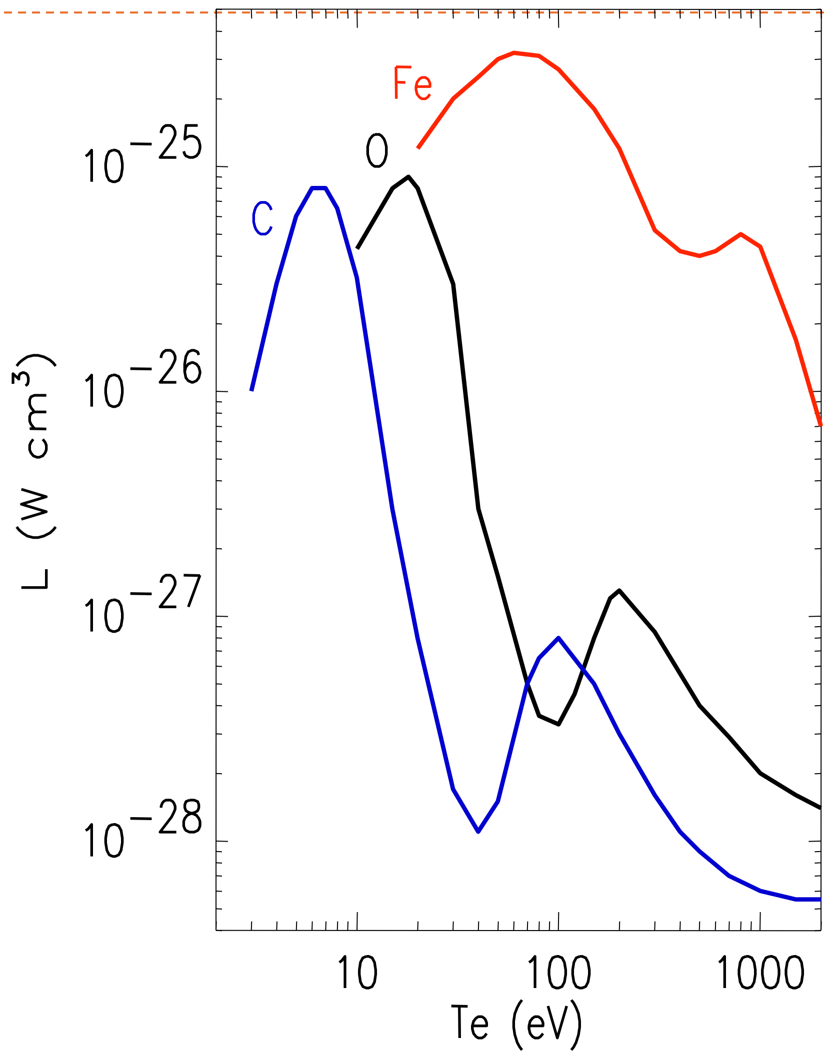

- Major impurities in LHD are C, O and Fe.
- Average-ion coronal-equilibrium model (ADPAC) for impurity radiation calculation

$$S_Z = n_Z n_e L_Z (T_e)$$

- C peaks at 6 eV
- O peaks at 20 eV
- Iron dominates lighter impurities for Te > 50eV
- let $L_{imp} = 10^{-25}$Wcm^3, n_{imp}=0.004n_e, P_{imp}=48kW

Conventional Technology – Resistive Bolometer

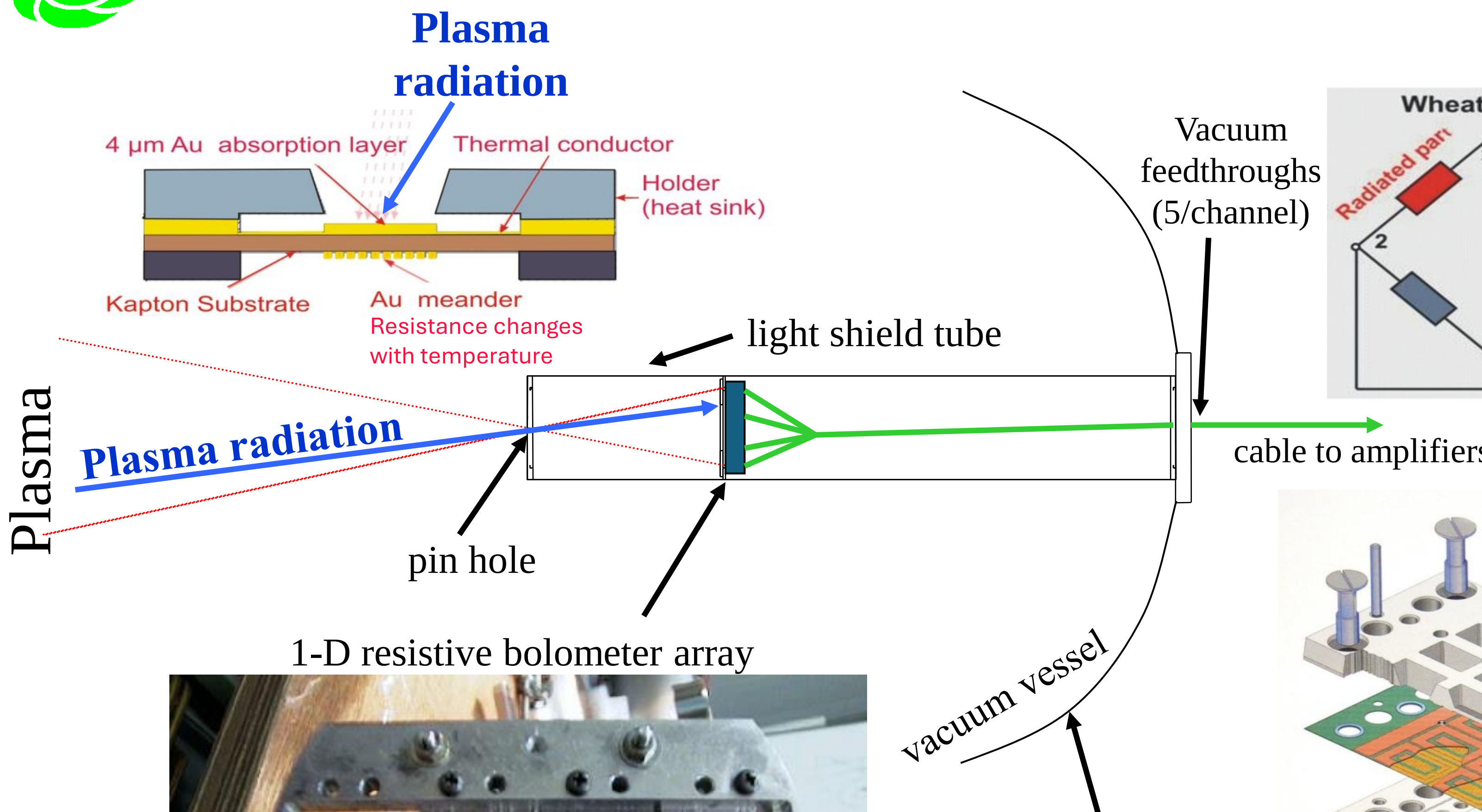

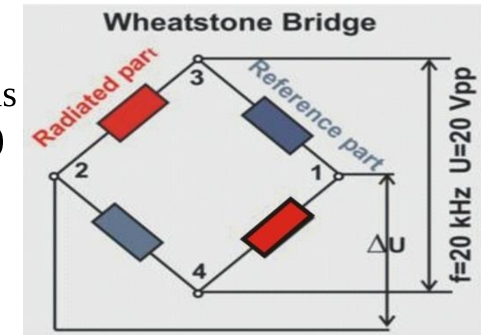

1-D resistive bolometer array

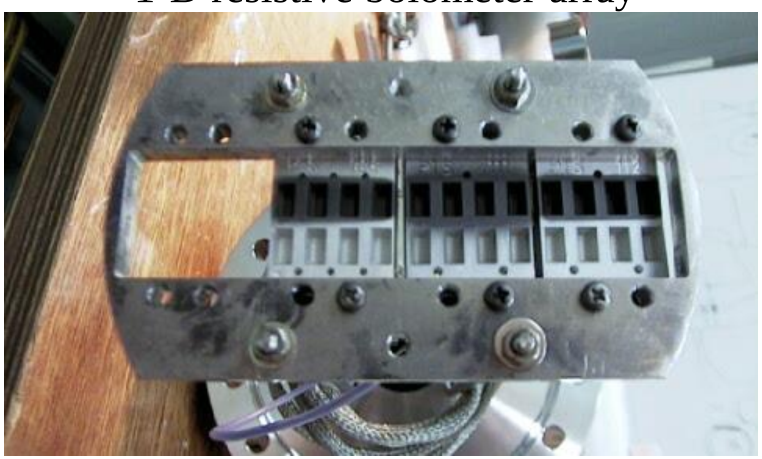

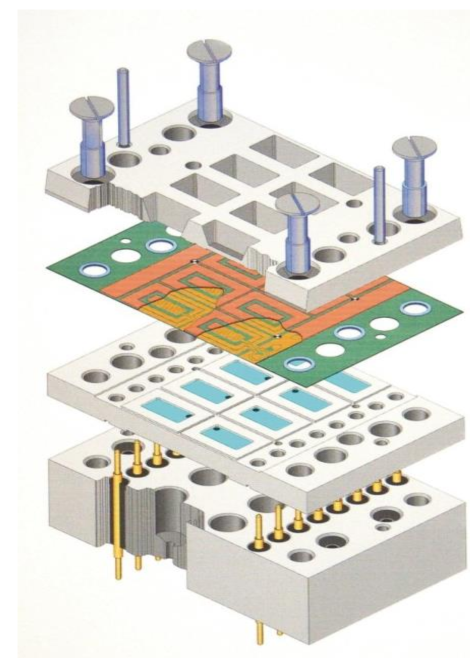

Providing reliable measurements since 1878! (S. P. Langley)

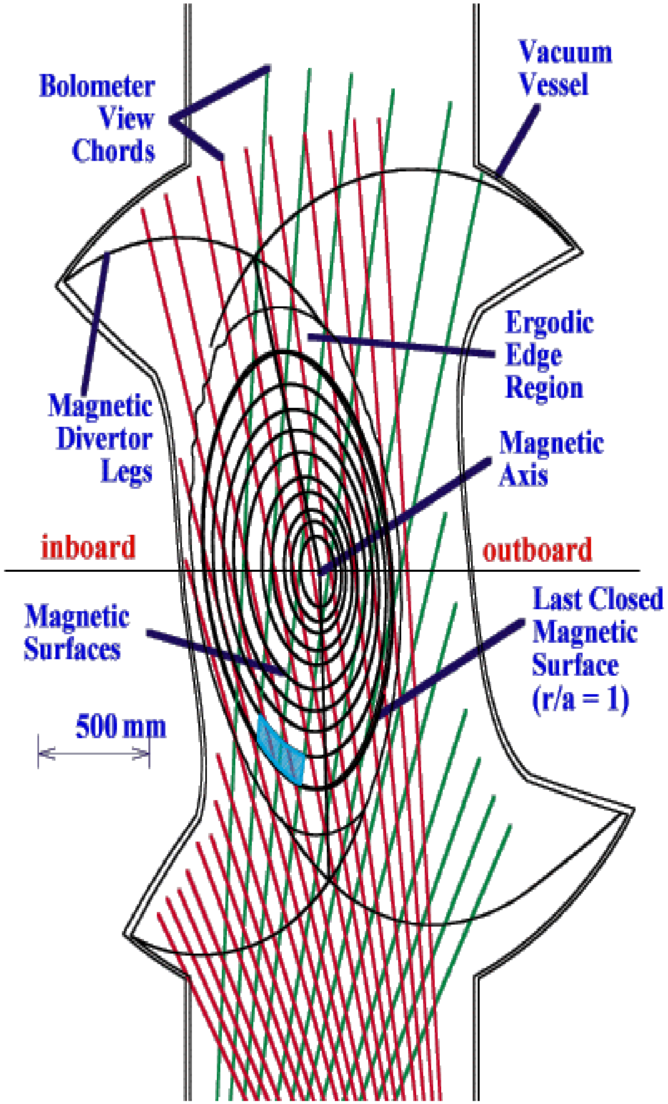

CAD drawing of bolometer sight lines and magnetic surfaces

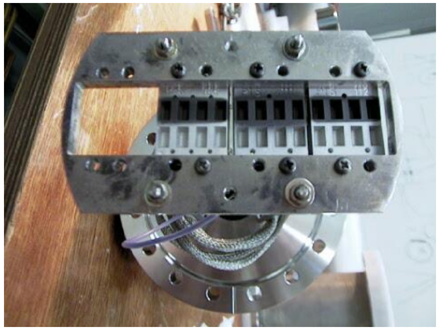

12 channel bolometer array

Detector

- Gold foil resistive bolometer
- Sensitivity ~ 20 μW/cm^2
- Blackened with Graphite
- Time resolution 10 ms
- 56 channels installed in LHD

Calibration

Calibrated with chopped HeNe laser of power, P_{rad}, and bolometer signal voltage, V_b, to determine sensitivity, K, and thermal time, τ, from

$$P_{rad} = \frac{1}{K}\left(V_b + \tau \frac{\partial V_b}{\partial t}\right)$$

Alternative - IR imaging Video Bolometer (IRVB)

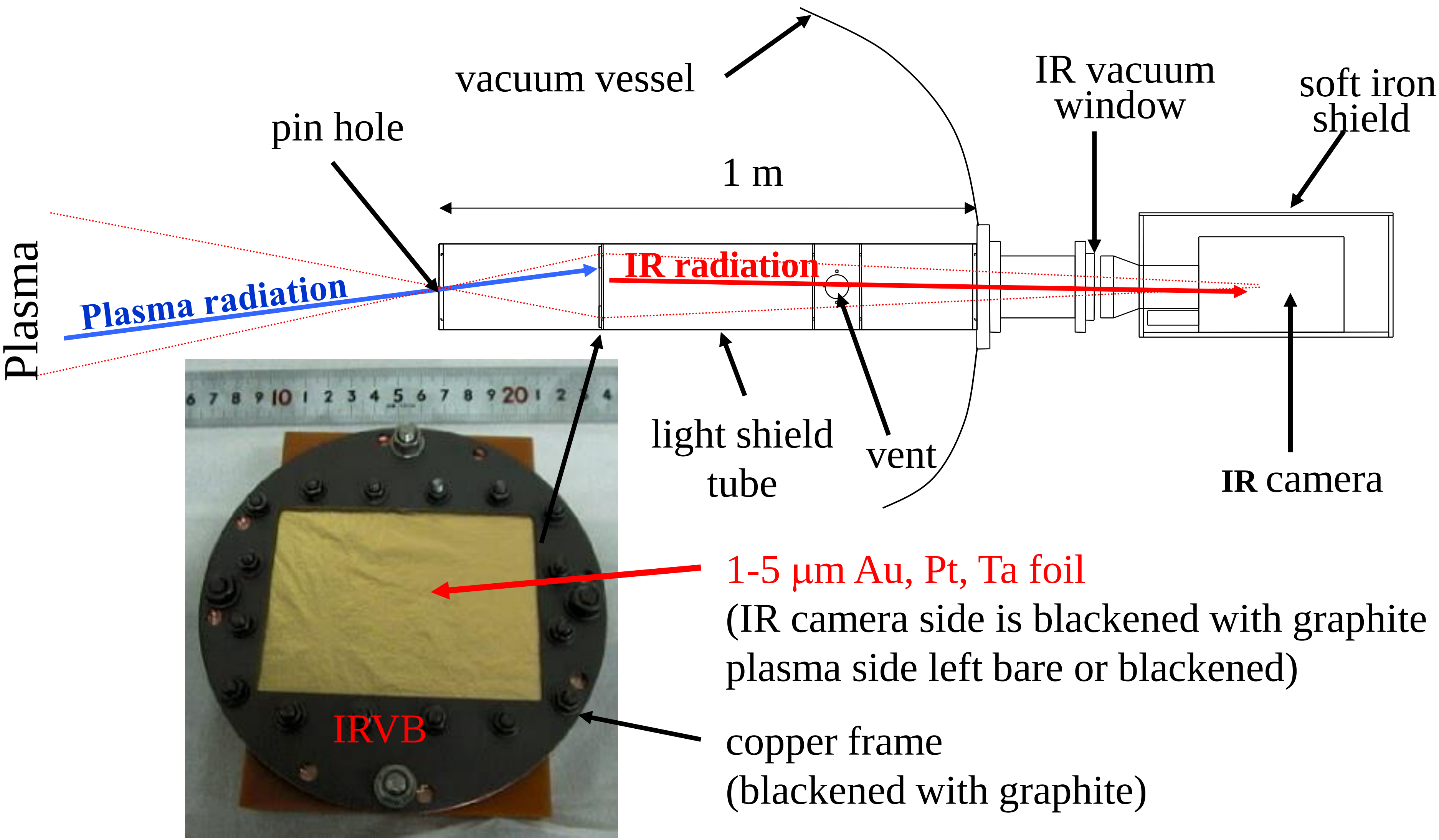

[1] B.J. Peterson, *Rev. Sci. Instrum.* **70** (2000) 3696. [2] B.J. Peterson *et al.*, *Rev. Sci. Instrum.* **72** (2001) 923.

IRVB - Concept

Solve foil 2D heat diffusion equation for P_{rad}

$$-\Omega_{rad} + \Omega_{bb} + \frac{1}{\kappa}\frac{\partial T}{\partial t} = \frac{\partial^2 T}{\partial x^2} + \frac{\partial^2 T}{\partial y^2}$$

foil thermal diffusivity

2-D Laplacian

$$\Omega_{bb} = \frac{\varepsilon \sigma_{S-B}(T^4 - T_0^4)}{k t_f} \qquad \varepsilon \cong 1$$

foil black body emissivity

foil thermal conductivity

black body cooling term

$$\Omega_{rad} = \frac{P_{rad}}{k t_f l^2}$$

plasma radiated power is determined by solving heat diffusion equation

foil thickness

bolometer pixel area

IRVB pinhole camera

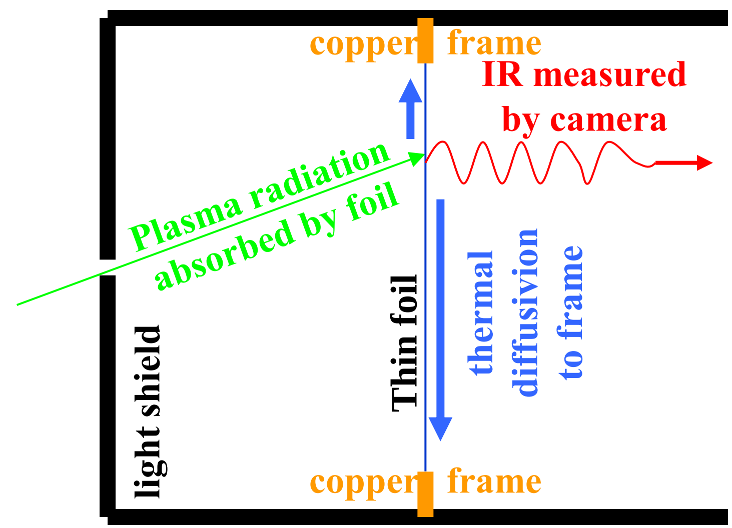

Using an implicit numerical scheme (Crank-Nicolson) to calculate spatial and temporal derivatives

B.J. Peterson *et al.*, *Rev. Sci. Instrum.* **74** (2003) 2040.

IRVB - Calibration

Solve foil power balance equation for P_{rad}

$$-\Omega_{rad} + \Omega_{bb} + \frac{1}{\kappa}\frac{\partial T}{\partial t} = \frac{\partial^2 T}{\partial x^2} + \frac{\partial^2 T}{\partial y^2}$$

2-D Laplacian

foil thermal diffusivity

foil black body emissivity

$$\Omega_{bb} = \frac{\varepsilon \sigma_{S-B}(T^4 - T_0^4)}{k t_f} \qquad \varepsilon \cong 1$$

black body cooling term

$$\Omega_{rad} = \frac{P_{rad}}{k t_f l^2}$$

plasma radiated power is determined by solving heat diffusion equation

foil thermal conductivity

foil thickness

bolometer pixel area

IRVB pinhole camera

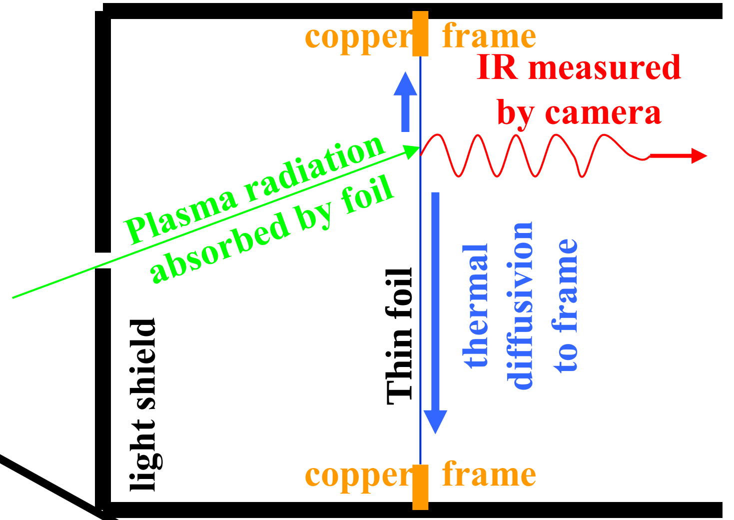

Parameters to be determined locally on the foil through calibration experiments with laser

B.J. Peterson *et al., Rev. Sci. Instrum.* **74** (2003) 2040.

Trade offs are important in diagnostic design

$$S_{IRVB} = \frac{\eta_{IRVB} N_{bol}}{A_f} = \frac{\sqrt{10} k t_f \sigma_{IR}}{\sqrt{f_{IR} N_{IR}}} \sqrt{\frac{N_{bol}^3 f_{bol}}{A_f^2} + \frac{N_{bol} f_{bol}^3}{5\kappa^2}}$$

Derived from foil power balance equation by propagation of IR camera T error, σ_{IR}.

~$20k ~$100k

Maker/ IR Camera	FLIR/ Omega (2)	FLIR/ SC500 (2)	FLIR/ A40-M	FLIR/ Phoenix (2)	FLIR/ SC4000	FLIR/ SC6000
λ (μm)	7.5-13.5	7.5-13	7.5-13	3-5	3-5	3-5
σ_{IR} (°C@ 30°C)	0.1	0.1	0.08	0.025	0.025	0.025
type	μ bolo	μbolo	μbolo	InSb	InSb	InSb
cooling style	none	none	none	Stirling	Stirling	Stirling
N_{IR}	160x 120	320x 240	320x 240	320x 256	320x 256	640x 512
f_{IR} (Hz)	30	60	60	345	420	125
*S_{IRVB} (μW/cm²)	441	156	125	16	14	13

* for IRVB with 16 x 12 ch, 30 Hz, l = .5625 cm, Au, t_f = 4 microns

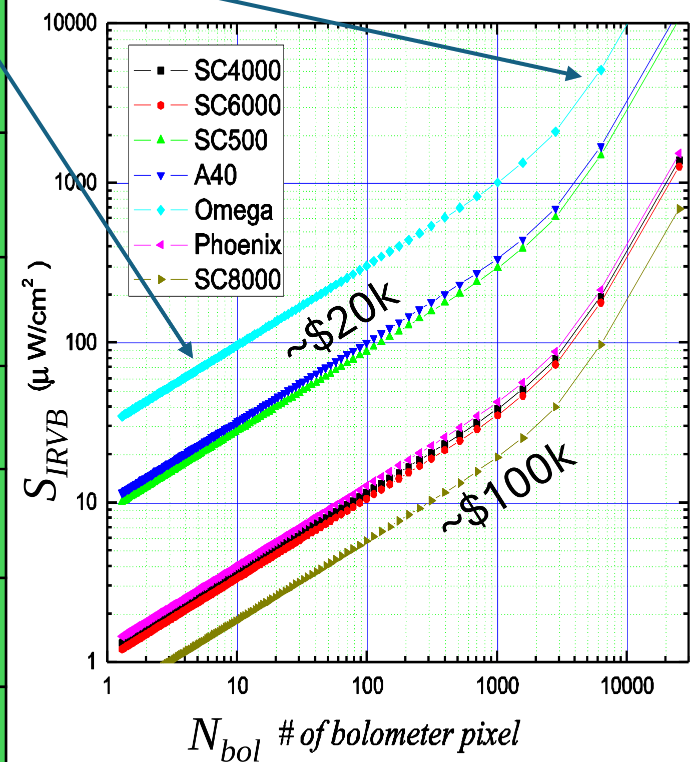

for Au IRVB foil with A_f=60.75 cm², t_f=4μm, f_{bol}=30/s

Gold Foil Thickness (sensitivity) vs Photon Energy

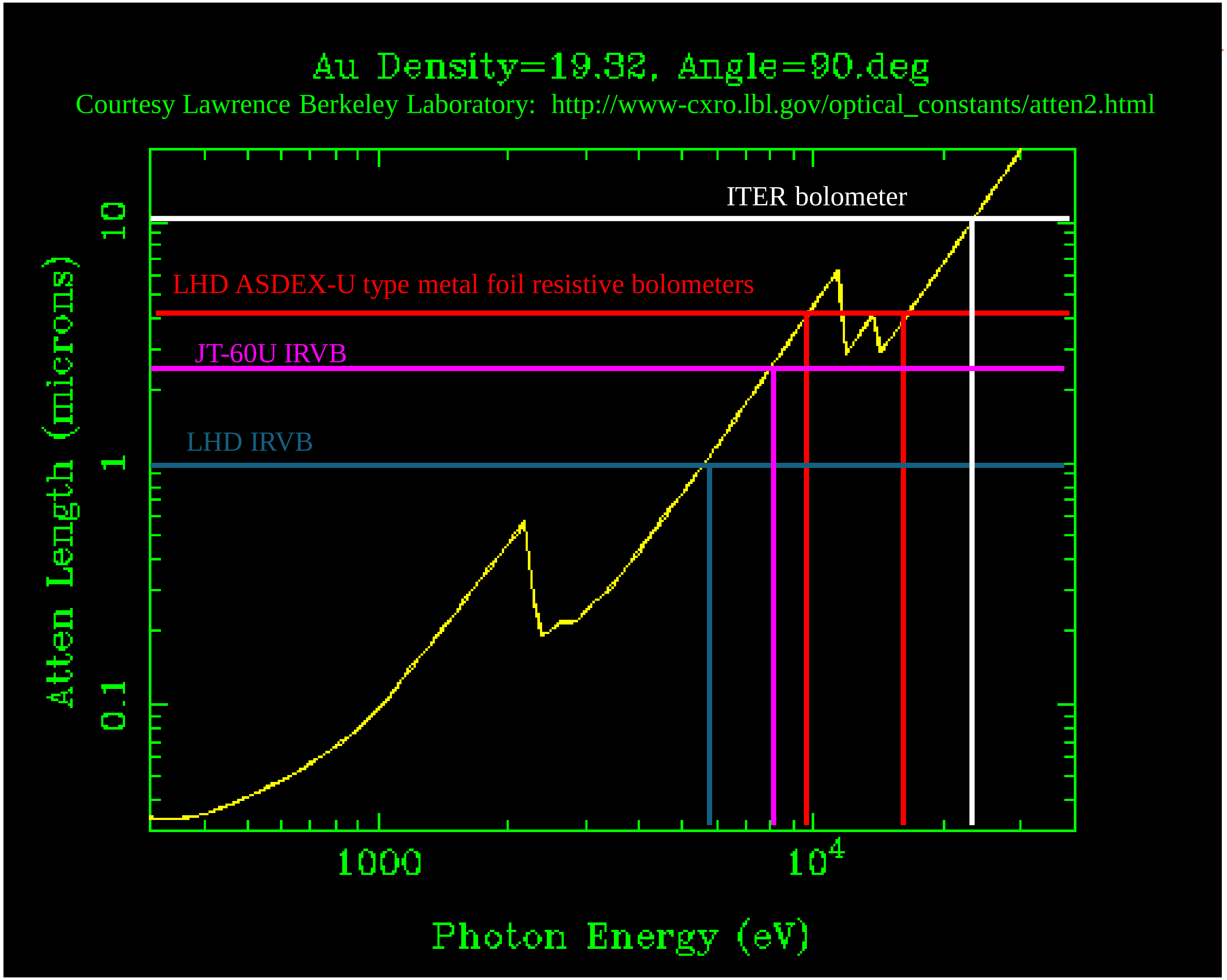

Outline

- Bolometer diagnostics
  - Sources of radiation
  - Resistive bolometers (RB)
  - Imaging bolometers (IRVB)
- Geometry matrix calculation
- Synthetic diagnostics
  - for comparison of plasma model with experimental data
  - utilization for diagnostic design
- Tomography examples:
  - 1D using SVD with RB in LHD
  - 2D using RGS with RB in W7-X
  - 2D using Phillips Tikhonov with 1 IRVB in KSTAR
  - 3D using Tikhonov with 4 IRVBs in LHD
  - 2D using SART and Bayesian with RBs and IRVB in MAST-U
- Conclusion

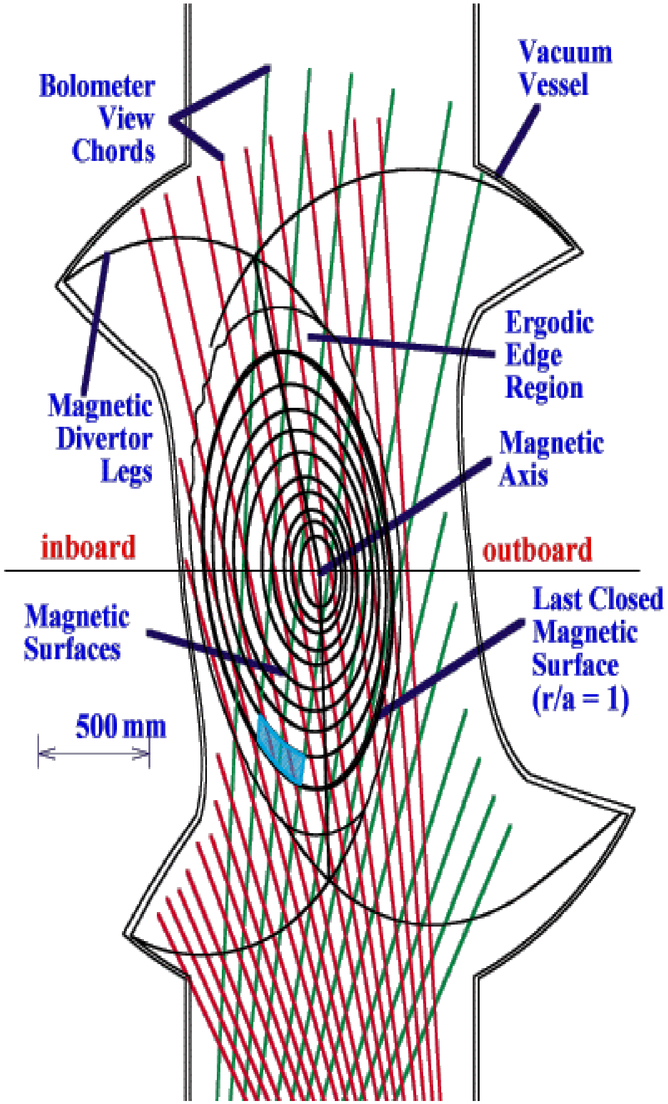

CAD drawing of bolometer sight lines and magnetic surfaces

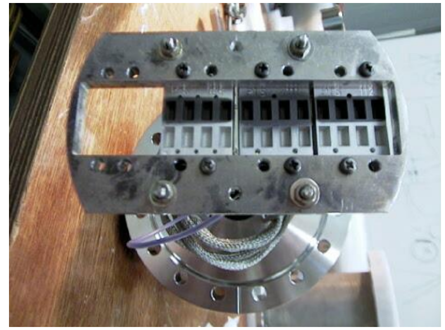

12 channel bolometer array

Detector

- Gold foil resistive bolometer
- Sensitivity ~ 20 μW/cm^2
- Blackened with Graphite
- Time resolution 10 ms
- 56 channels installed in LHD

Calibration

Calibrated with chopped HeNe laser of power, P_{rad}, and bolometer signal voltage, V_b, to determine sensitivity, K, and thermal time, τ, from

$$P_{rad} = \frac{1}{K}\left(V_b + \tau \frac{\partial V_b}{\partial t}\right)$$

Profile Inversion

- β = 0.32 magnetic surfaces (black in figure) included in CAD model with bolometer sight lines (red and green)
- Surfaces divided by lines between x-points and axis
- Calculate intersection of viewing chord volume and inter-surface volume, V_{ij}, and solid angles, Ω_{ij}. Write system of equations for detector power, P_i, and volume emissivity, S_j

$$P_i = \sum_j \frac{\Omega_{ij}}{4\pi} V_{ij} S_j = \sum_j T_{ij} S_j$$

- Invert geometry matrix, T_{ij}, using Singular Value Decomposition
- Back substitute with singularities removed to solve for S_j

1D plasma grid definition

assumption: constant on a flux surface

$$P_i = \sum_j \frac{\Omega_{ij}}{4\pi} V_{ij} S_j = \sum_j T_{ij} S_j$$

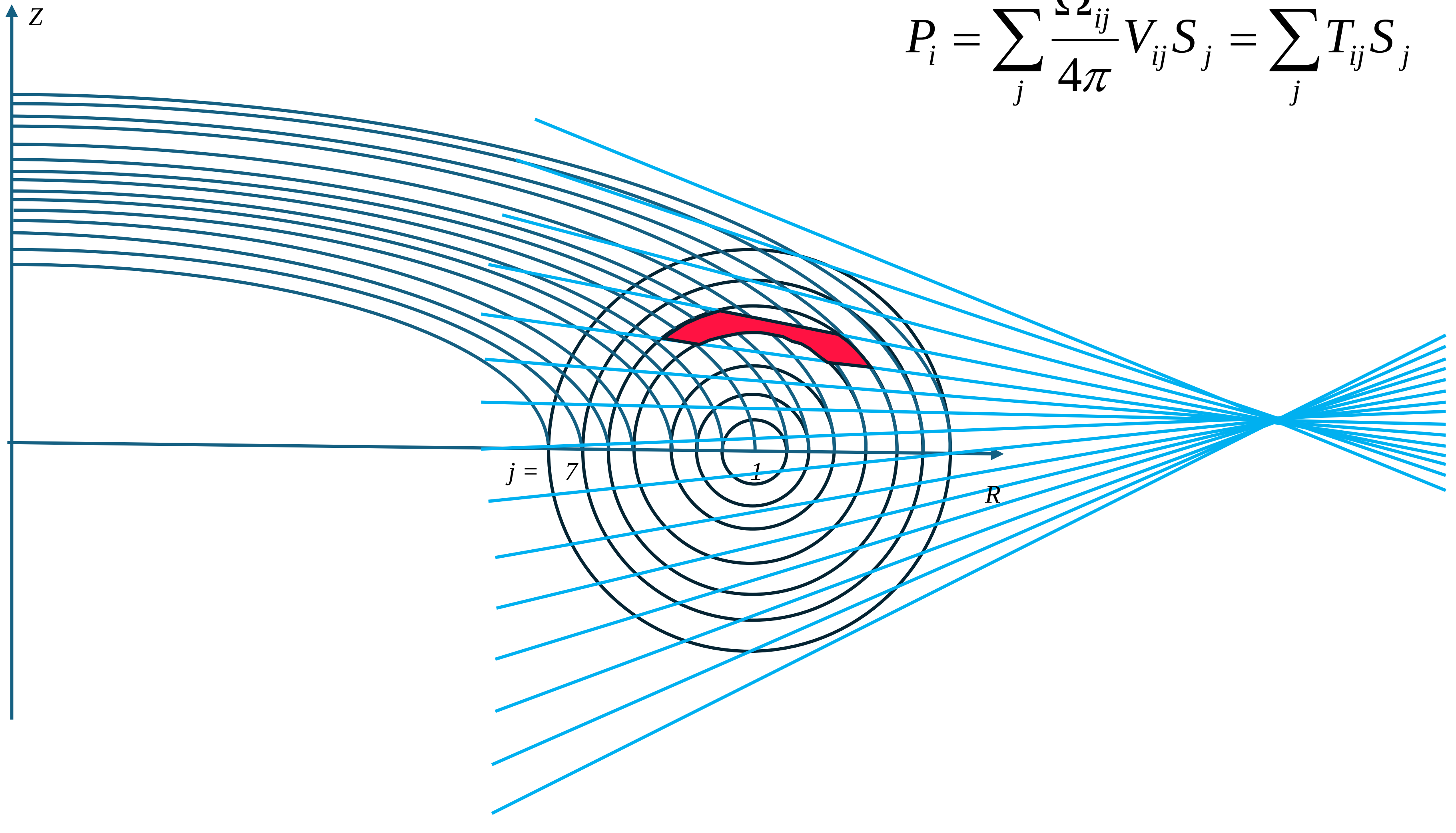

2D plasma grid definition

assumption: axisymmetry

$$P_i = \sum_j \frac{\Omega_{ij}}{4\pi} V_{ij} S_j = \sum_j T_{ij} S_j$$

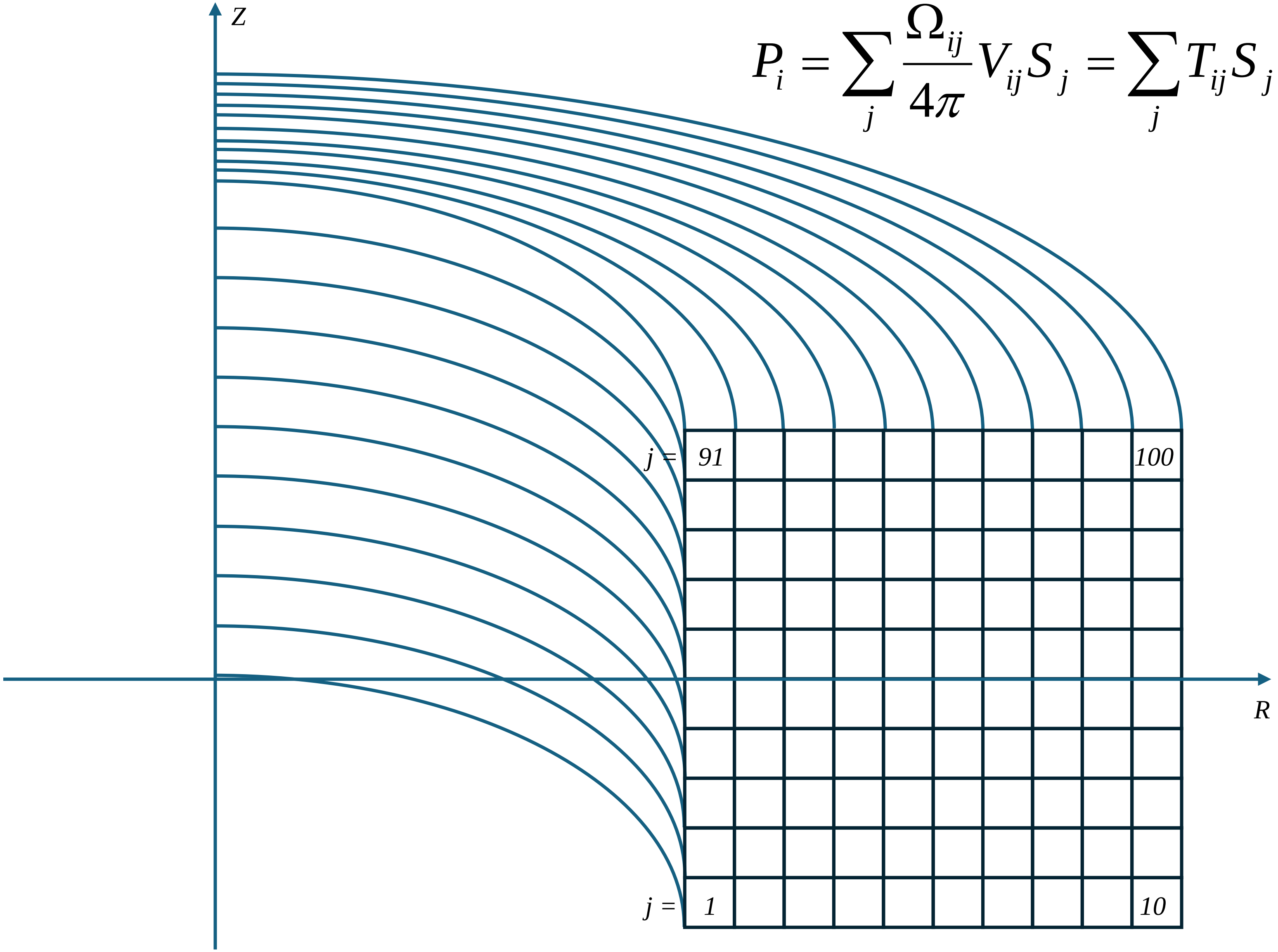

3D plasma grid definition

assumption: non axisymmetric but constant in a finite volume

$$P_i = \sum_j \frac{\Omega_{ij}}{4\pi} V_{ij} S_j = \sum_j T_{ij} S_j$$

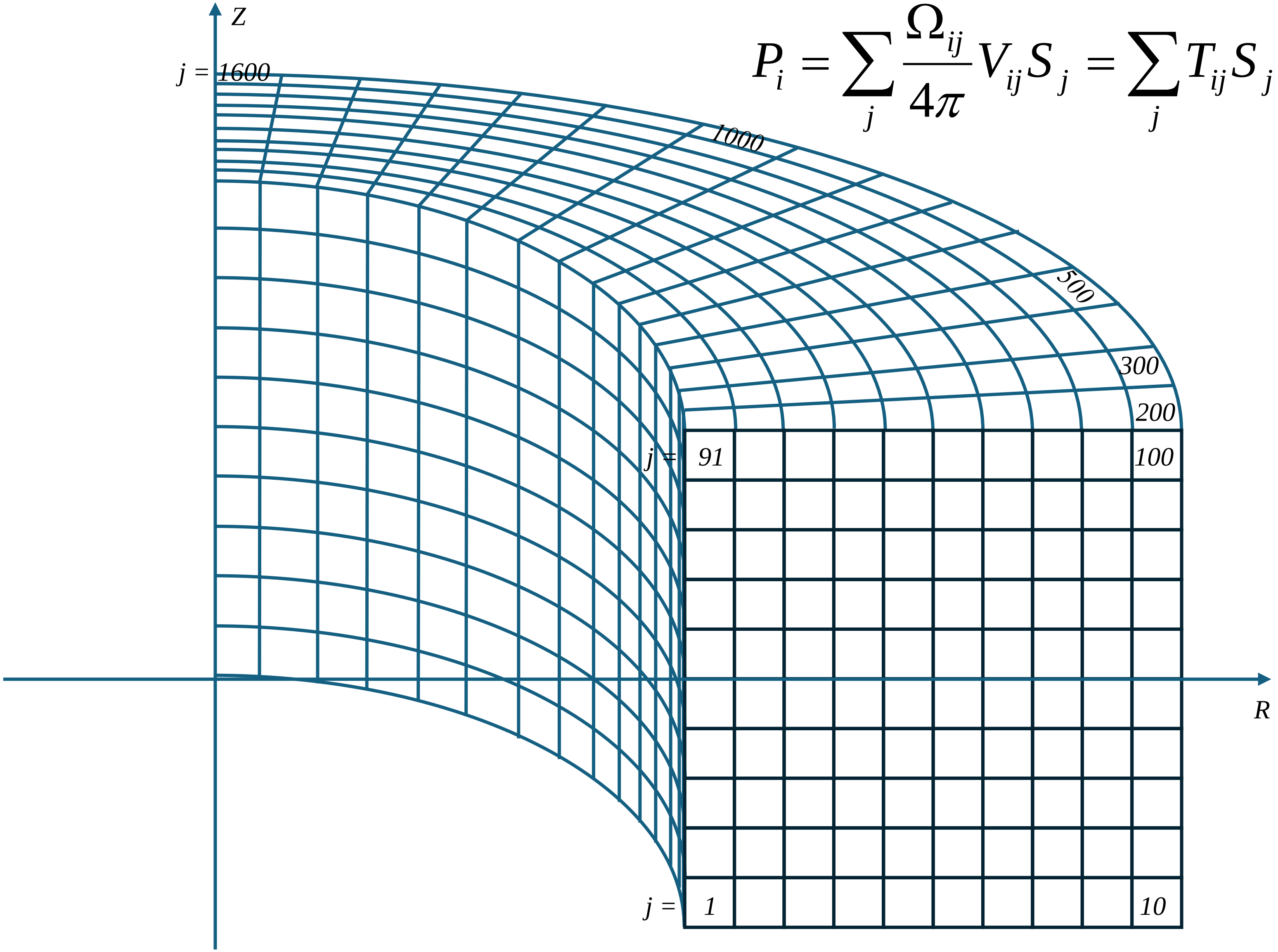

2D Geometry matrix calculation

Tomography converts line-integrated data into a local measurement

$$P_i = \sum_j \frac{\Omega_{ij}}{4\pi} V_{ij} S_j = \sum_j T_{ij} S_j$$

$$\Omega_{i,j} / 4\pi = A_i / A_{Si,j}$$

$$\Omega_{i,j} / 4\pi = A_i / 4\pi \, l_{i,j}^2$$

$$A_{Si,j} = 4\pi \, l_{i,j}^2$$

$$T_{i,j} = V_{i,j} \Omega_{i,j} / 4\pi = V_{i,j} A_i / 4\pi \, l_{i,j}^2$$

$$T_{23,36} = V_{23,36} \, A_{23} / 4\pi \, l_{23,36}^2$$

Need to also consider:

- *effective area of detector* ($\cos\theta$)
- *Effective area of aperture* ($\cos\theta$)
- *finite area of detector*
- *finite area of aperture*
- *wall reflections?*
- *others?*

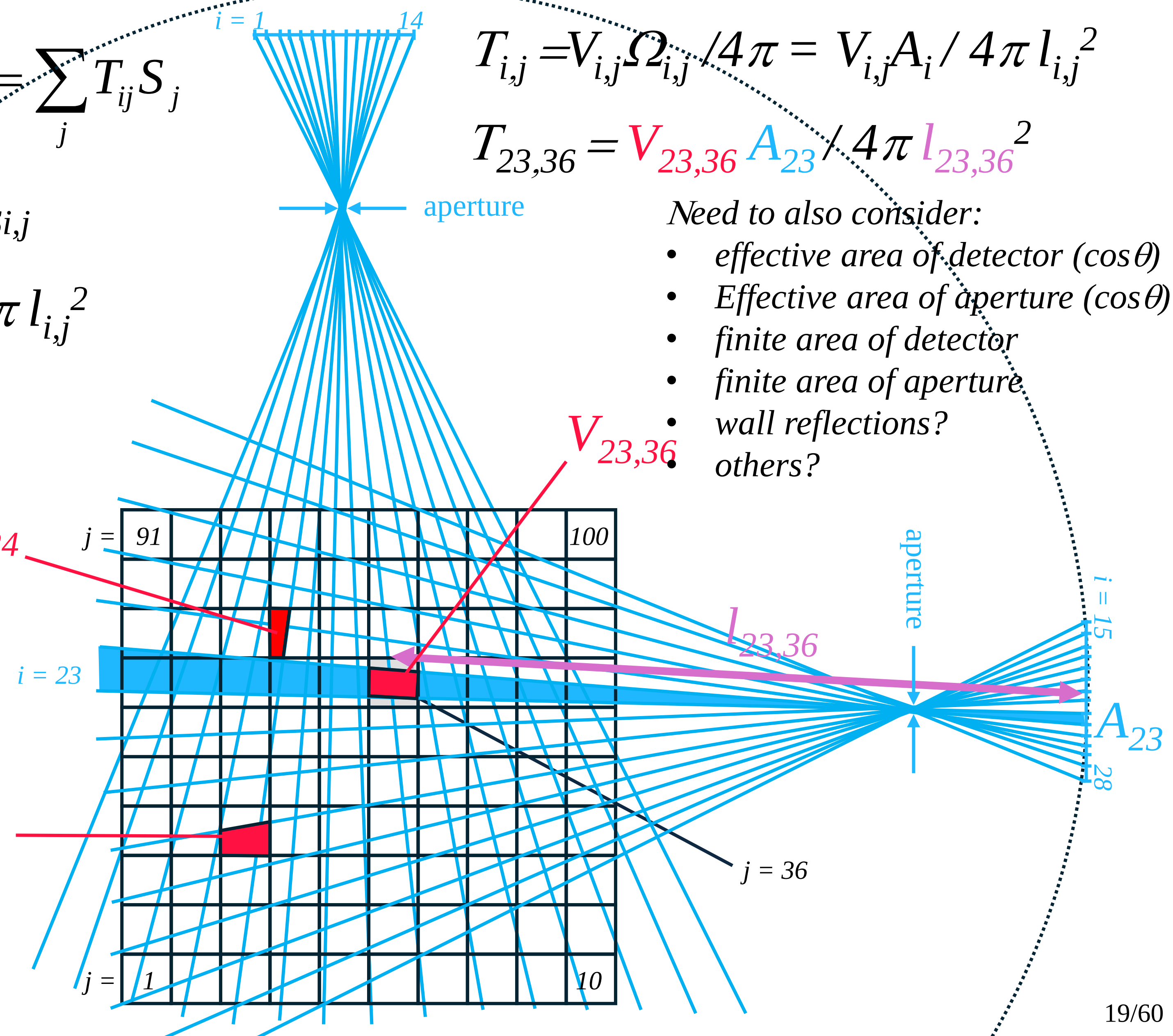

Advanced techniques use CHERAB with Raysect ray tracing package

Resistive Bolometer Arrays, Calibration and Profile Inversion

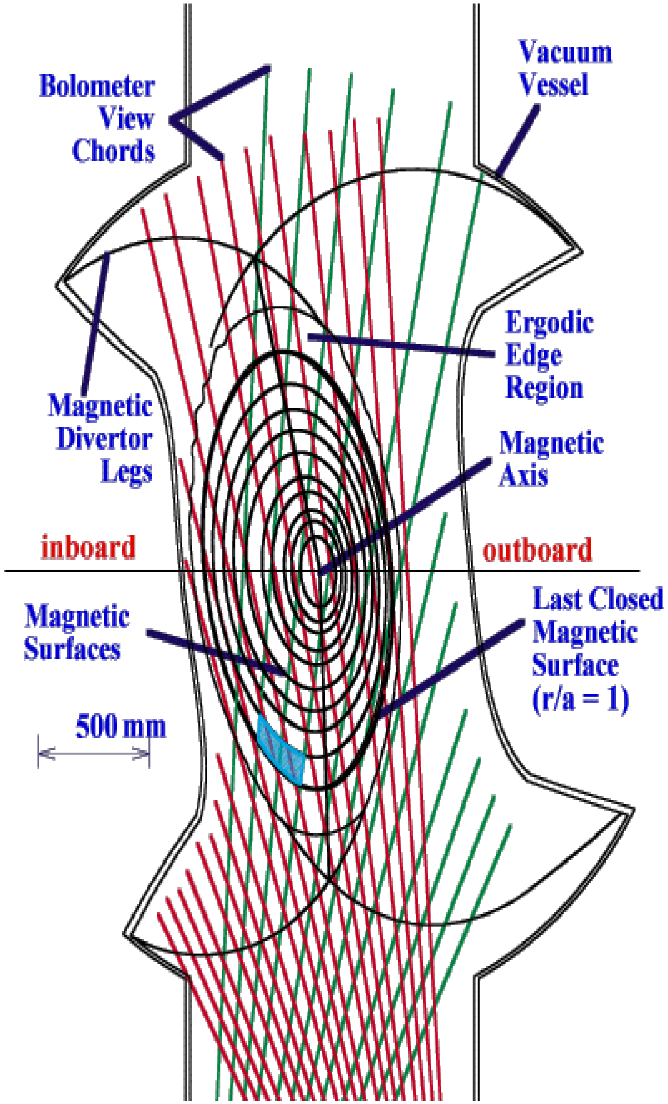

CAD drawing of bolometer sight lines and magnetic surfaces

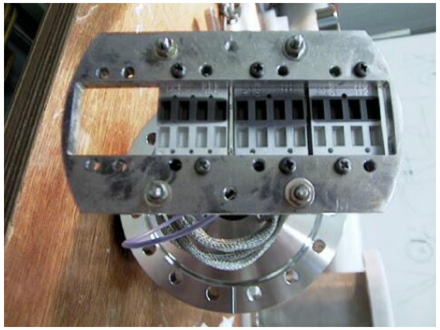

12 channel bolometer array

Detector

- Gold foil resistive bolometer
- Sensitivity ~ 20 μW/cm^2
- Blackened with Graphite
- Time resolution 10 ms
- 56 channels installed in LHD

Calibration

Calibrated with chopped HeNe laser of power, P_{rad}, and bolometer signal voltage, V_b, to determine sensitivity, K, and thermal time, τ, from

$$P_{rad} = \frac{1}{K}\left(V_b + \tau \frac{\partial V_b}{\partial t}\right)$$

Profile Inversion

- β = 0.32 magnetic surfaces (black in figure) included in CAD model with bolometer sight lines (red and green)
- Surfaces divided by lines between x-points and axis
- Calculate intersection of viewing chord volume and inter-surface volume, V_{ij}, and solid angles, Ω_{ij}. Write system of equations for detector power, P_i, and volume emissivity, S_j

$$P_i = \sum_j \frac{\Omega_{ij}}{4\pi} V_{ij} S_j = \sum_j T_{ij} S_j$$

- Invert geometry matrix, T_{ij}, using Singular Value Decomposition
- Back substitute with singularities removed to solve for S_j

Outline

- Bolometer diagnostics
  - Sources of radiation
  - Resistive bolometers (RB)
  - Imaging bolometers (IRVB)
- Geometry matrix calculation
- Synthetic diagnostics
  - for comparison of plasma model with experimental data
  - utilization for diagnostic design
- Tomography examples:
  - 1D using SVD with RB in LHD
  - 2D using RGS with RB in W7-X
  - 2D using Phillips Tikhonov with 1 IRVB in KSTAR
  - 3D using Tikhonov with 4 IRVBs in LHD
  - 2D using SART and Bayesian with RBs and IRVB in MAST-U
- Conclusion

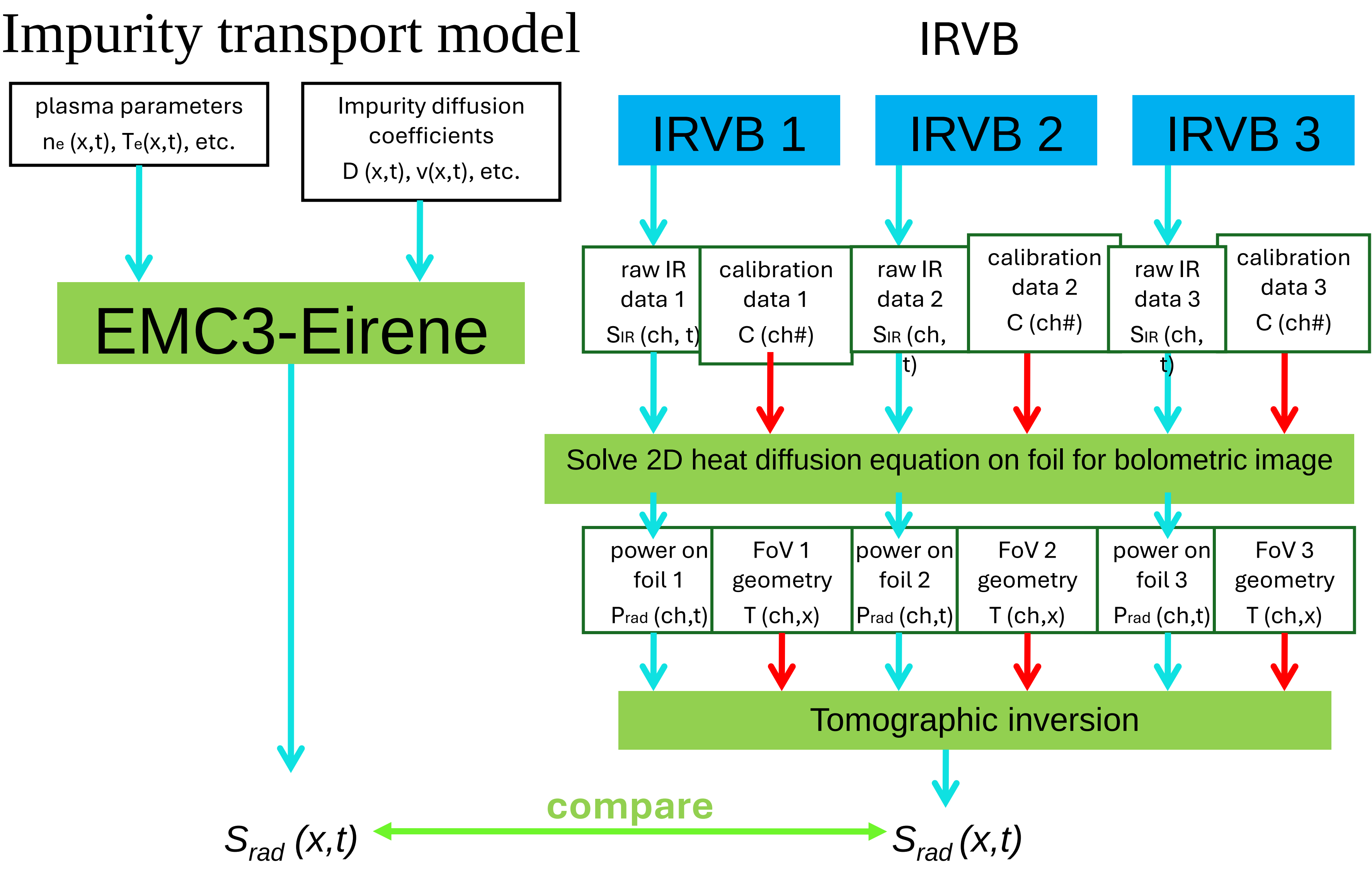
Impurity transport model
IRVB
plasma parameters
ne (x,t), Te(x,t), etc.
Impurity diffusion coefficients
D (x,t), v(x,t), etc.
EMC3-Eirene
IRVB 1
IRVB 2
IRVB 3
raw IR data 1
SIR (ch, t)
calibration data 1
C (ch#)
raw IR data 2
SIR (ch, t)
calibration data 2
C (ch#)
raw IR data 3
SIR (ch, t)
calibration data 3
C (ch#)
Solve 2D heat diffusion equation on foil for bolometric image
power on foil 1
Prad (ch,t)
FoV 1 geometry
T (ch,x)
power on foil 2
Prad (ch,t)
FoV 2 geometry
T (ch,x)
power on foil 3
Prad (ch,t)
FoV 3 geometry
T (ch,x)
Tomographic inversion
Srad (x,t)
compare
Srad (x,t)

Imaging bolometer: Using foil temperature distribution to solve heat diffusion equation for radiated power image

IRVB experimental data

Foil temperature from IR camera

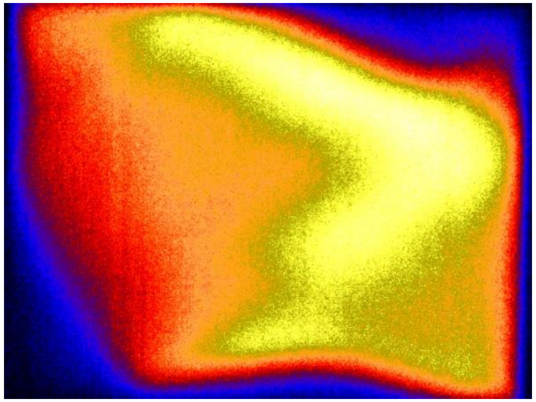

Spatial variation of thermal and surface properties like kt_f, κ and ε obtained from foil calibration

Solving 2D heat diffusion equation on foil

$$S_{rad} = S_{bb} + \frac{1}{\kappa}\frac{\partial T}{\partial t} - \left[\frac{\partial^2 T}{\partial x^2} + \frac{\partial^2 T}{\partial y^2}\right]$$

gives experimental IRVB image

$$P_{rad} = S_{rad} A_{bol}$$

Power on foil, P_{rad}

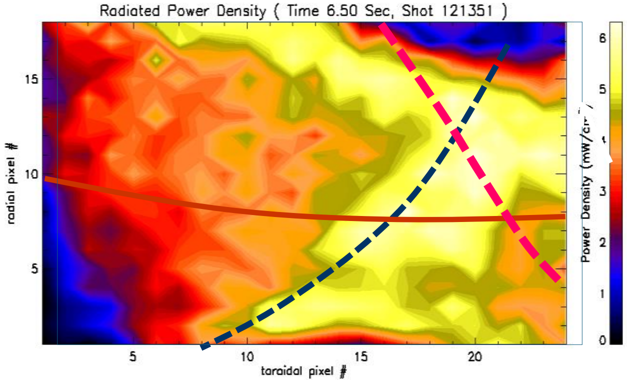

Synthetic instrument: a means to establish comparison with experiments

Modeling

Plasma parameters $n_e(x,t)$, $T_e(x,t)$, *etc.*	*Impurity diffusion coefficients* $D(x,t)$, $v(x,t)$, *etc.*

EMC3-EIRENE

3D edge carbon radiation estimate

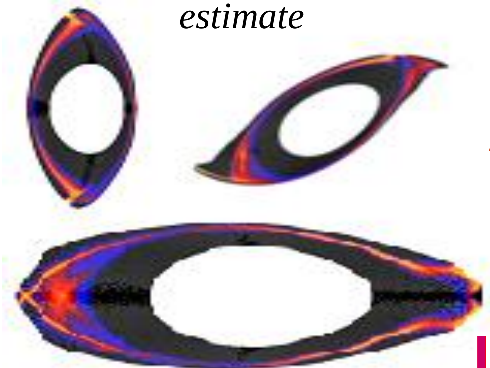

S_j

Field of View

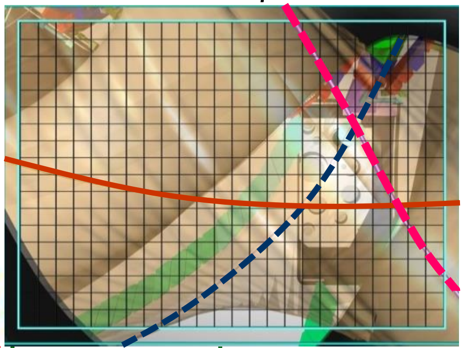

Geometry matrix

$$T_{ij} = \frac{\Omega_{ij}}{4\pi} V_{ij}$$

Synthetic image

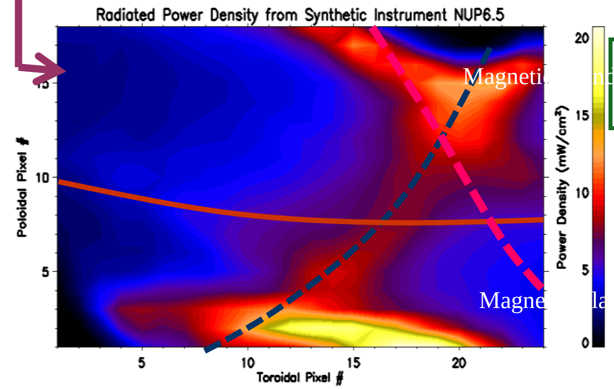

Power at foil, P_{rad}

$$P_i = \sum_j T_{ij} S_j$$

Synthetic instrument:
a means to establish a comparison between model and experiment

IRVB experimental data

Foil temperature from IR camera

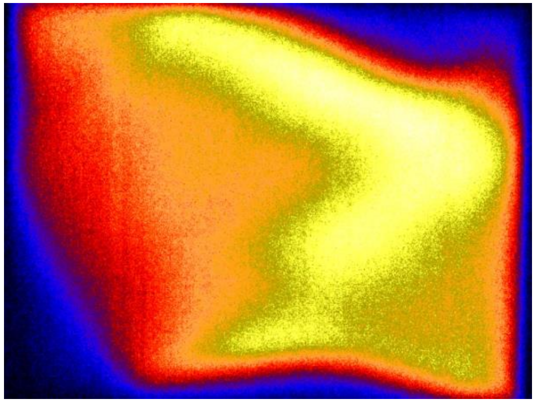

Spatial variation of thermal and surface properties like kt_f, κ and ε obtained from foil calibration

Solving 2D heat diffusion equation on foil

$$S_{rad} = S_{bb} + \frac{1}{\kappa}\frac{\partial T}{\partial t} - \left[\frac{\partial^2 T}{\partial x^2} + \frac{\partial^2 T}{\partial y^2}\right]$$

gives experimental IRVB image

$$P_{rad} = S_{rad} A_{bol}$$

Power on foil, P_{rad}

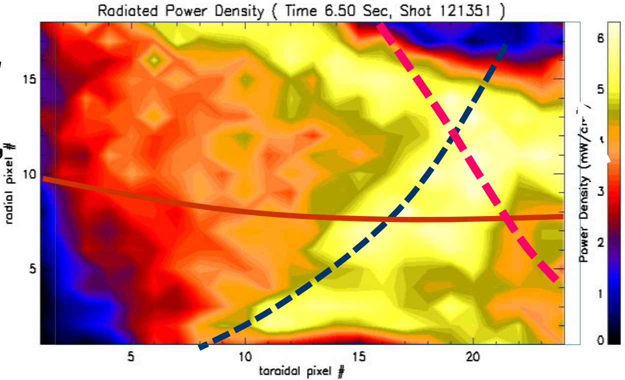

directly compare

Modeling

Plasma parameters
n_e (x,t), T_e(x,t), etc.

Impurity diffusion coefficients
D (x,t), v(x,t), etc.

EMC3-EIRENE

3D edge carbon radiation estimate

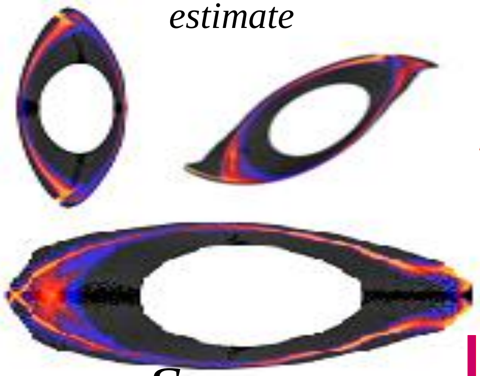

S_j

Field of View

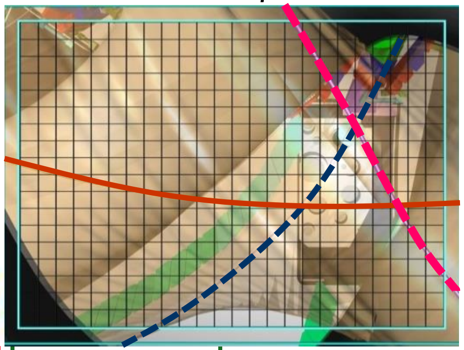

Response matrix

$$T_{ij} = \frac{\Omega_{ij}}{4\pi} V_{ij}$$

Synthetic image

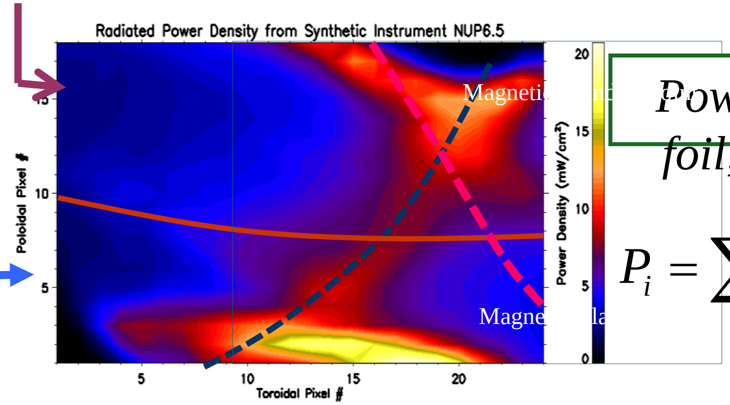

Power at foil, P_{rad}

$$P_i = \sum_j T_{ij} S_j$$

Calculating synthetic images from plasma models

- SANCO provides S(ρ) in 30 annular regions
- SOLPS provides S(R,Z) in 8866 cells
- Models for the following case are considered:
  - Fuel , 2% Be, 10^{-5} W
- SANCO and SOLPS P_{rad} data resampled:
  - 2 cm R,Z grid 219 (R) x 465 (Z) voxels
- 2 IRVB cases are considered:
  - Tangential view of full cross-section:
    - IR camera 512 x 640, 15 mK, 1000 f/s
    - 15x20 pixels, aperture 6 x 6 mm^2
  - Zoomed view of divertor
    - IR camera 1024 x 1280, 15 mK, 105 f/s
    - 24x32 pixels, aperture 3.75 x 3.75 mm^2
- Projection matrices, H, calculated
  - by 3D integration along sight lines
  - Divided into sub-apertures
  - To keep < 2 cm integration cells
- Synthetic images calculated from:

$$P_i = \sum_j H_{ij} S_j$$

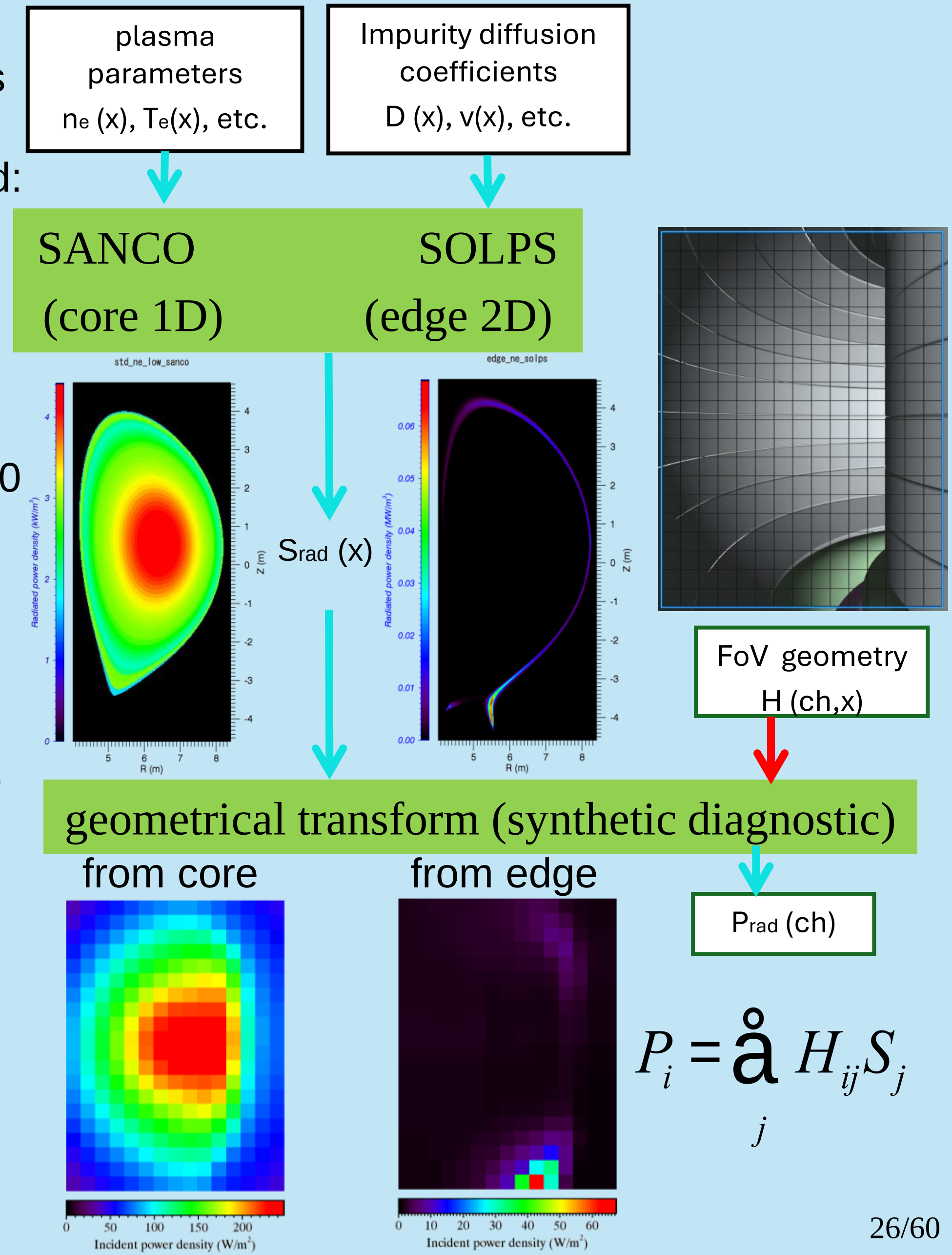

Power spectra shows high energy x-rays from core

- for full cross-section IRVB: 15 x 20 (h x v) pixels
  - aperture (x,y,z) = (-5619.042, -6474.626, 470)
  - foil (x,y,z) = (-5619.042, -6552.626, 470)
  - (R=8572.89) (mm) (same as 12L IR system)

- SANCO and SOLPS data are provided in terms of both spatial location and photon energy [5]

$S_j = S\,(x,E)$ 1 eV < E < 100 keV (236 channels)

- Using the projection matrix for the IRVB the power spectrum, $P_i(E)$, for each IRVB channel is calculated.

$$P_i = \sum_j H_{ij} S_j$$

- This is reduced to 93 energy channels from 1.1 to 97.8 keV
- Power spectra is plotted for 4 channels on mid-plane

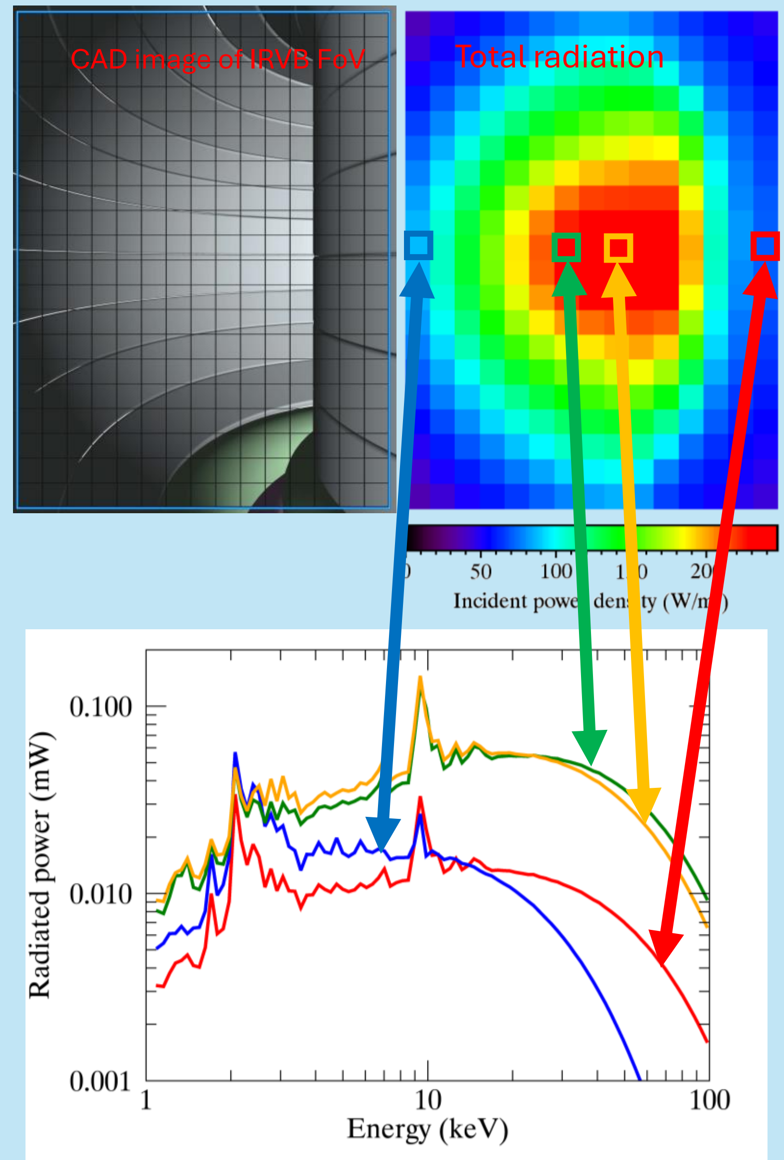

[5] https://user.iter.org/?uid=RTPL2V

Calculating necessary foil thickness

- Necessary foil thickness should be determined before S/N is calculated
- SANCO and SOLPS data are provided in terms of both spatial location and photon energy [5]

$S_j = S\,(x,E)$ 1 eV < E < 100 keV (236 channels)

- Using the projection matrix for the IRVB the power spectrum, $P_i(E)$, for each IRVB channel is calculated.

$$P_i = \sum_j H_{ij} S_j$$

- Mass attenuation coefficient, $\mu/\rho(E)$, from NIST [6] is used to calculate the fraction of the incident power, $P/P_0(t_f)$, absorbed by a Pt foil of thickness, t_f, and mass density, ρ.

$$\frac{P}{P_0}(t_f) = \frac{1}{P_0}\sum\nolimits_E P(E)\left\{1 - e^{-\frac{\mu}{\rho}(E)\rho t_f/\cos\theta}\right\}$$

- Incident angle, θ, of sight line with respect to foil is considered to calculate effective thickness of foil, where $\theta = 0$ is considered normal incidence.

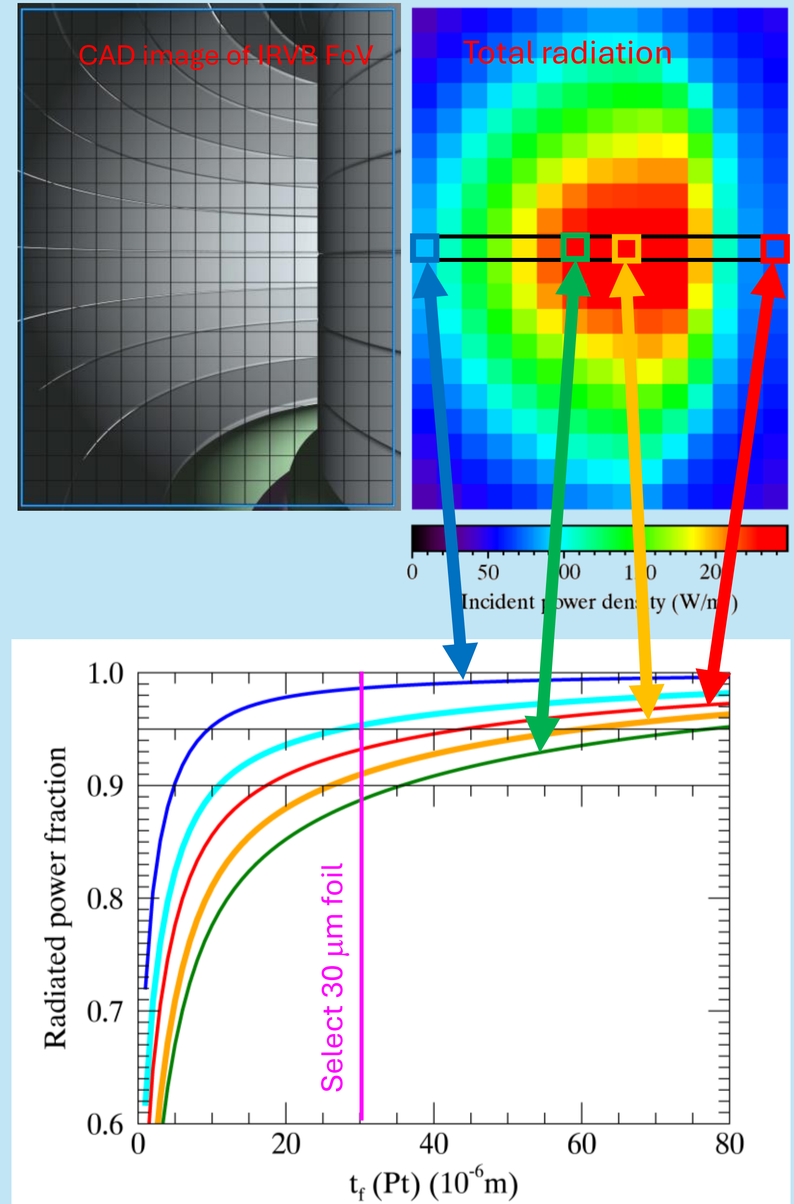

[5] https://user.iter.org/?uid=RTPL2V
[6]https://physics.nist.gov/PhysRefData/XrayMassCoef/chap2.html

Necessary foil thickness for core IRVB on ITER

$$\frac{P}{P_0}(t_f)=\frac{1}{P_0}\sum_E P(E)\left\{1-e^{-\frac{\mu}{\rho}(E)\rho t_f/\cos\theta}\right\}$$

For core viewing IRVB

- Maximum energy channel (green)
  - 90% of P_{rad} absorbed by 36 μm Pt foil
  - 95% of P_{rad} absorbed by 78 μm Pt foil
- Maximum power channel (orange)
  - 90% of P_{rad} absorbed by 27 μm Pt foil
  - 95% of P_{rad} absorbed by 61 μm Pt foil
- Inboard channel (like resistive bolometer) (red)
  - 90% of P_{rad} absorbed by 18 μm Pt foil
  - 95% of P_{rad} absorbed by 45 μm Pt foil
- Outboard channel (blue)
  - 90% of P_{rad} absorbed by 5 μm Pt foil
  - 95% of P_{rad} absorbed by 10 μm Pt foil
- Total foil (cyan)
  - 90% of P_{rad} absorbed by 11 μm Pt foil
  - 95% of P_{rad} absorbed by 28 μm Pt foil

Select 30 μm Pt foil

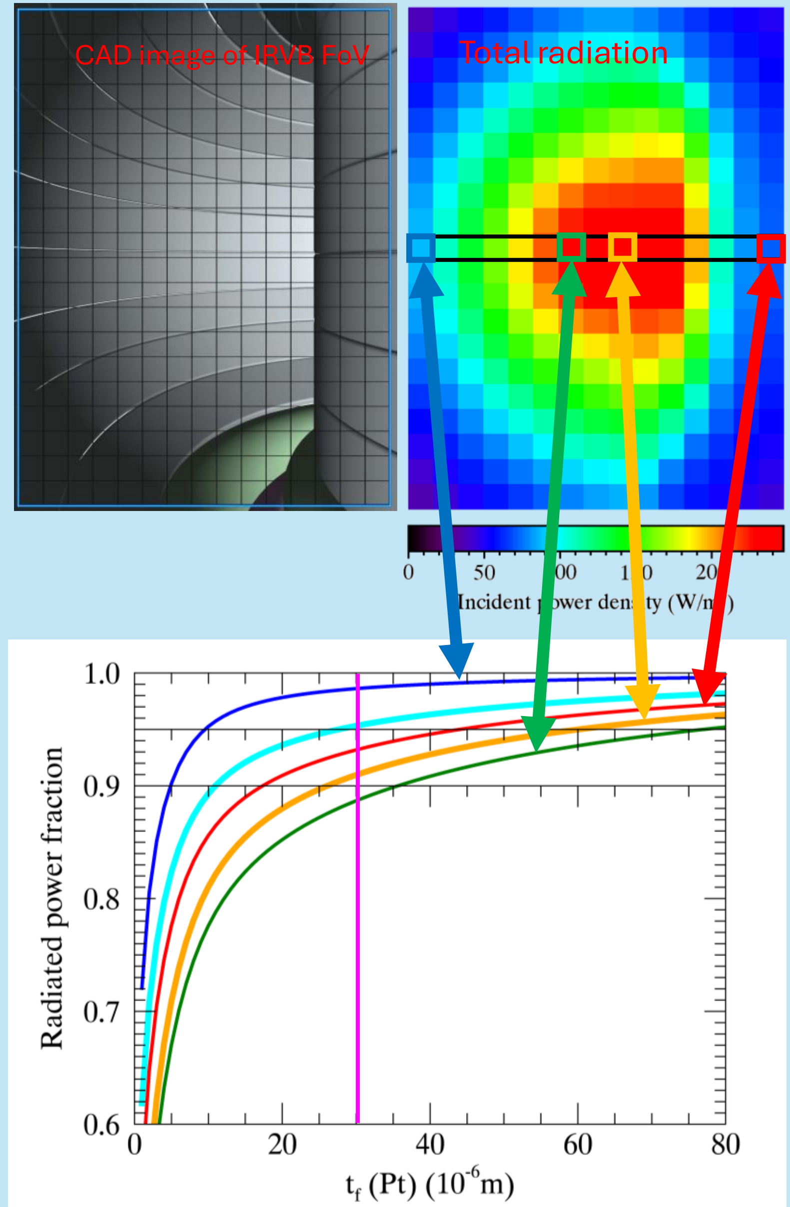

Estimation of noise and signal (roughly)

.

~0

$$S_{IRVB} = \frac{\eta_{IRVB} N_{bol}}{A_f} = \frac{\sqrt{10} k t_f \sigma_{IR}}{\sqrt{f_{IR} N_{IR}}} \sqrt{\frac{N_{bol}^3 f_{bol}}{A_f^2} + \frac{N_{bol} f_{bol}^3}{5\kappa^2}} \quad [4]$$

$$S_{signal} = \frac{P_{signal}}{A_{bol}} = \frac{A_{bol} A_{ap} \cos^4 J P_{rad} l_{plasma}}{A_{bol} 4 p l_{ap-f}^2 V_{plasma}}$$

Foil properties (Pt):
k = 0.716 W/cmK – foil thermal cond.
κ = 0.2506 cm^2/s – foil thermal diffusivity
t_f – foil thickness
A_f = 48 cm^2 – utilized area of the foil
IR camera properties:
σ_{IR} = 15 mK – IR camera NET
f_{IR} – frame rate of IR camera
N_{IR} – number of IR pixels
IRVB properties:
A_{bol} – pixel area
f_{bol} – frame rate of IRVB
N_{bol} – # of bolometer pixels
S_{IRVB} – IRVB noise equivalent power density
η_{IRVB} – IRVB noise equivalent power

Plasma parameters:
L_{plasma} = 10 m – length sight line in plasma
P_{rad} = 67.27 MW – total radiated power
V_{plasma} = 1049 m^3 – plasma volume
Pinhole camera properties:
$A_{ap} = 2.25 * A_{bol}$ – area of aperture
$l_{ap\text{-}f}$ – distance from foil to aperture
Θ = 10,20 – angle between sightline and aperture
S_{signal} – estimated radiated power density on foil
$S/N = S_{signal}/S_{IRVB}$ – signal to noise ratio

[4] B.J. Peterson *et al.*, *Rev. Sci. Instrum.* **74** (2003) 2040.

$$SNR = \frac{S_{signal}}{S_{IRVB}} = \frac{\kappa \cos^4 \vartheta P_{rad} l_{plasma}}{4\pi k t_f \sigma_{IR} l_{ap-f}^2 V_{plasma}} \sqrt{\frac{f_{IR} N_{IR} A_{bol}^3}{2 A_f f_{bol}^3}} = \frac{\kappa \cos^4 \vartheta P_{rad} l_{plasma} A_{ap}}{4\pi k t_f \sigma_{IR} l_{ap-f}^2 V_{plasma}} \sqrt{\frac{f_{IR} N_{IR}}{2 N_{bol} f_{bol}^3}}$$

IRVB parameters and S/N

IRVB	units	Core viewing IRVB					Divertor viewing IRVB			
IR camera parameters										
N_{pix}		512 × 640			1024 × 1280		512 × 640		1024 × 1280	
f_{IR}	1/s	1000			105		1000		105	
IRVB parameters										
t_f	μm	30					10			
$l_{ap\text{-}f}$	cm	7.8					21.0			
N_{IR}		327,680			1,310,720		327,680		1,310,720	
N_{bol}		15 × 20		24 × 32	15 × 20	24 × 32	15 × 20	24 × 32	15 × 20	24 × 32
t_{bol}	ms	10	1		10		1		10	
A_{bol}	mm^2	16		6.25	16	6.25	16	6.25	16	6.25
A_{ap}	mm^2	36		14.1	36	14.1	36	14.1	36	14.1
S_{IRVB}	W/m^2	2.07	65.3	105	3.19	5.12	21.5	34.5	1.05	1.69
Signal levels and signal to noise ratios										
S_{signal}	W/m^2	235	235	91.9	235	91.9	19.6	7.65	19.6	7.65
S/N		**114**	**3.6**	**0.88**	**73.8**	**18**	**0.91**	**0.22**	**18.6**	**4.53**
S_{core}	W/m^2	245	245	-	245	-	18.3	7.78	18.3	7.78
S_{edge}	W/m^2	67	67	-	67	-	49.7	29.2	49.7	29.2
S_{total}	W/m^2	246	246	-	246	-	61.8	34.4	61.8	34.4
S/N		**119**	**3.8**	**-**	**77**	**-**	**2.9**	**1.0**	**59**	**20**
		D2c	**D2b**	**D1b**	**D2a**	**D1a**	**E2b**	**E1b**	**E2a**	**E1a**

Outline

- Bolometer diagnostics
  - Sources of radiation
  - Resistive bolometers (RB)
  - Imaging bolometers (IRVB)
- Geometry matrix calculation
- Synthetic diagnostics
  - for comparison of plasma model with experimental data
  - utilization for diagnostic design
- Tomography examples:
  - 1D using SVD with RB in LHD
  - 2D using RGS with RB in W7-X
  - 2D using Phillips Tikhonov with 1 IRVB in KSTAR
  - 3D using Tikhonov with 4 IRVBs in LHD
  - 2D using SART and Bayesian with RBs and IRVB in MAST-U
- Conclusion

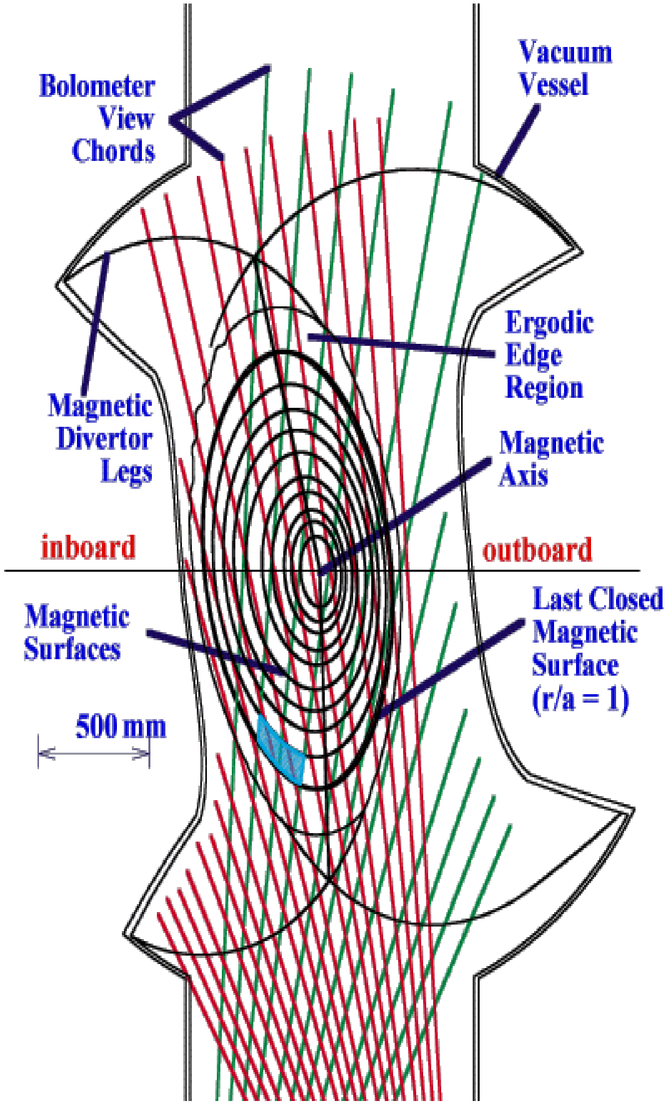

CAD drawing of bolometer sight lines and magnetic surfaces

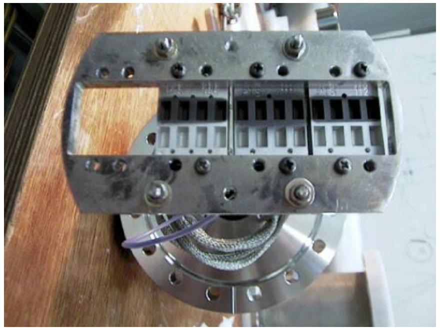

12 channel bolometer array

Detector

- Gold foil resistive bolometer
- Sensitivity ~ 20 μW/cm^2
- Blackened with Graphite
- Time resolution 10 ms
- 56 channels installed in LHD

Calibration

Calibrated with chopped HeNe laser of power, P_{rad}, and bolometer signal voltage, V_b, to determine sensitivity, K, and thermal time, τ, from

$$P_{rad} = \frac{1}{K}\left(V_b + \tau \frac{\partial V_b}{\partial t}\right)$$

Profile Inversion

- β = 0.32 magnetic surfaces (black in figure) included in CAD model with bolometer sight lines (red and green)
- Surfaces divided by lines between x-points and axis
- Calculate intersection of viewing chord volume and inter-surface volume, V_{ij}, and solid angles, Ω_{ij}. Write system of equations for detector power, P_i, and volume emissivity, S_j

$$P_i = \sum_j \frac{\Omega_{ij}}{4\pi} V_{ij} S_j = \sum_j T_{ij} S_j$$

- Invert geometry matrix, T_{ij}, using Singular Value Decomposition
- Back substitute with singularities removed to solve for S_j

Singular Value Decomposition

'SVD is also the method of choice for solving most linear least squares problems' – W.Press et al. in *Numerical Recipes*

$$\begin{pmatrix} P_1 \\ . \\ . \\ . \\ P_M \end{pmatrix} = \begin{pmatrix} T_{1,1} & T_{...,1} & T_{N,1} \\ . & ... & . \\ T_{1,.} & ... & . \\ . & ... & . \\ T_{1,M} & ... & T_{N,M} \end{pmatrix} \begin{pmatrix} S_1 & ... & S_N \end{pmatrix}$$

$$\begin{pmatrix} T_{1,1} & T_{...,1} & T_{N,1} \\ . & ... & . \\ T_{1,.} & ... & . \\ . & ... & . \\ T_{1,M} & ... & T_{N,M} \end{pmatrix} = \begin{pmatrix} U_{1,1} & U_{...,1} & U_{N,1} \\ . & ... & . \\ U_{1,...} & ... & . \\ . & ... & . \\ U_{1,M} & ... & U_{N,M} \end{pmatrix} \bullet \begin{pmatrix} w_1 & & \\ & w_{...} & \\ & & w_N \end{pmatrix} \bullet \begin{pmatrix} V_{1,1} & ... & V_{N,1} \\ . & V_{...} & . \\ V_{1,N} & ... & V_{N,N} \end{pmatrix}^T$$

P – power of M detectors
S – power density of N volumes
T – M x N geometry matrix

U – M x N column orthonormal matrix
V – N x N orthonormal matrix
w – N x N diagonal weighting matrix

Remove singularities – if w is small replace it by infinity!

$$\begin{pmatrix} S \end{pmatrix} = \begin{pmatrix} V \end{pmatrix} \bullet \begin{pmatrix} 1/w \end{pmatrix} \bullet \begin{pmatrix} U \end{pmatrix}^T \bullet \begin{pmatrix} P \end{pmatrix}$$

C – confidence in inversion $C_j = \sqrt{\sum_{i=1}^{M} \frac{V_{ij}^2}{w_j^2}}$

σ_{in} – instrumental error

$$\begin{pmatrix} \sigma_{Sin} \end{pmatrix} = \begin{pmatrix} V \end{pmatrix} \bullet \begin{pmatrix} 1/w \end{pmatrix} \bullet \begin{pmatrix} U \end{pmatrix}^T \bullet \begin{pmatrix} \sigma_{Pin} \end{pmatrix}$$

Combining instrumental error and inversion confidence for total error:

$$\sigma_{Sj} = \sqrt{\left(S_j C_j\right)^2 + \sigma_{S_{in}j}^2}$$

1D tomographic inversion - sample

Initial line-averaged brightness data P_i, (with error bars) is used with SVD to invert geometry matrix and get local emissivity, S_j.

As a check, S_j is then multiplied by the geometry matrix to get the detector data, $P_{i\ inv}$.

If this falls between the error bars of the original P_i measurement, then the inversion should be valid.

$$P_i = \sum_j \frac{\Omega_{ij}}{4\pi} V_{ij} S_j = \sum_j T_{ij} S_j$$

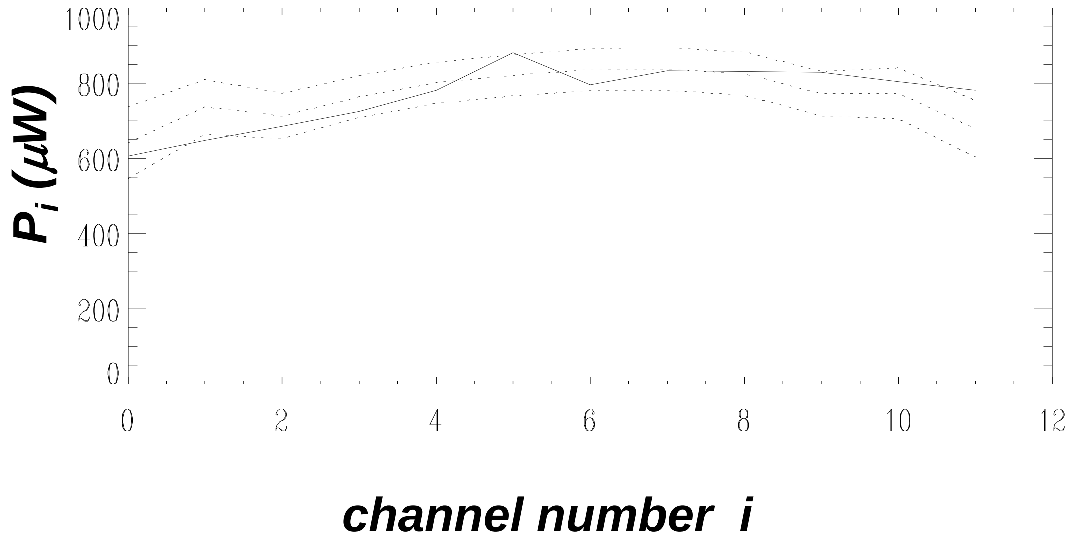

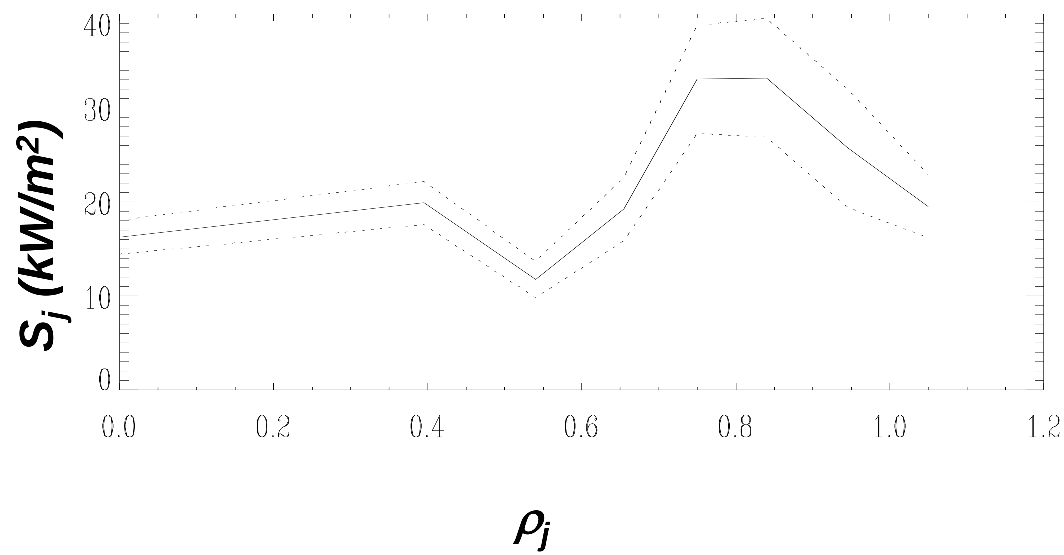

2D tomography in W7-X with resistive bolometer arrays

- 65 lines of sight (bolometer channels)
  - In 2 cameras at triangular x-section
- Plasma grid based on VMEC equilibrium:
  - 200 poloidal x 29 radial, $n_p > 2000$
- Inversion technique:
  - Relative Gradient Smoothing

$$P_i = \sum_j \frac{\Omega_{ij}}{4\pi} V_{ij} S_j = \sum_j T_{ij} S_j$$

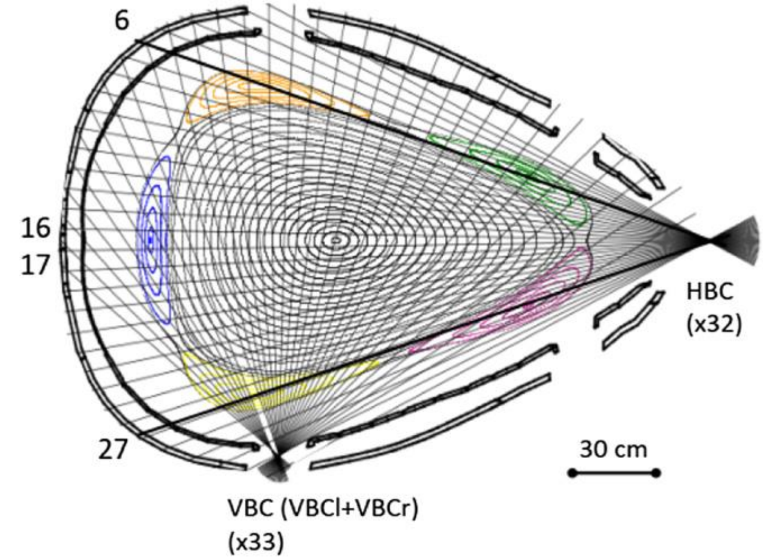

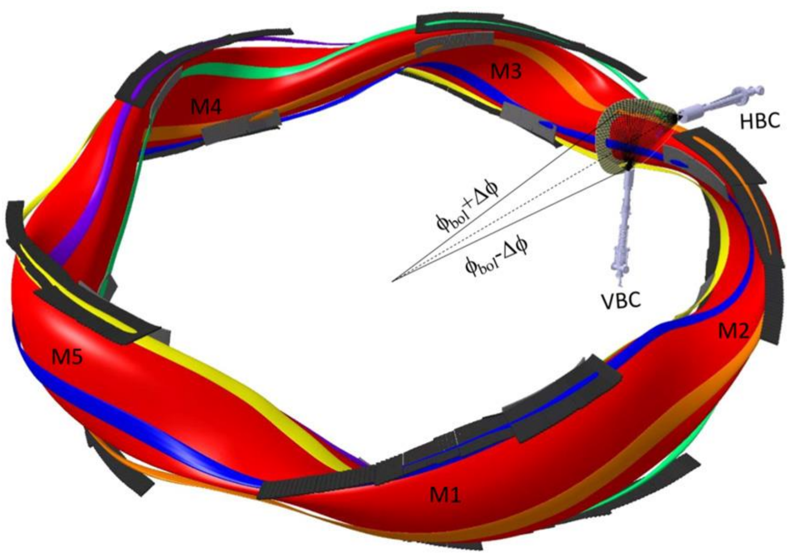

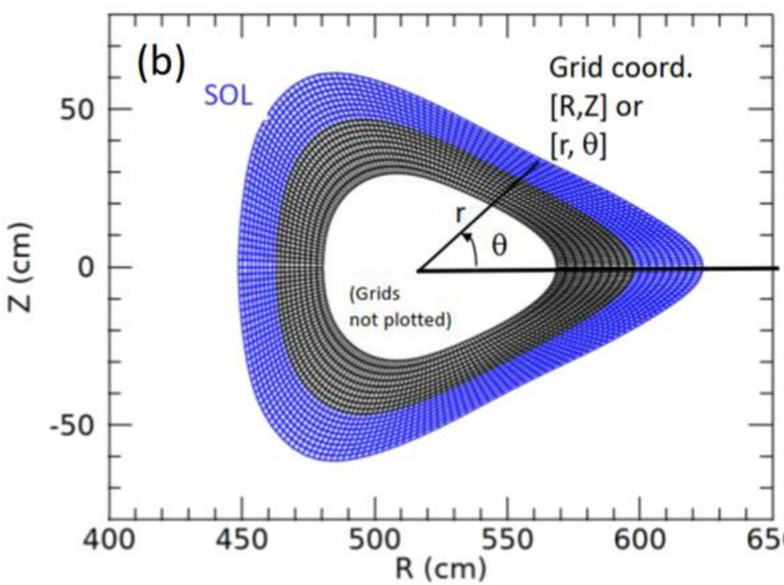

D. Zhang et al., Nucl. Fusion **61** (2021) 116043

Geometry matrix calculation in W7-X

Using a series of line-integrated measurements:

$$P_l = \int \varepsilon \left[\frac{\cos(\alpha)\cos(\beta) A_D A_S}{4\pi d^2}\right] ds, \qquad l = 1, \dots, n_l - 1$$

camera etendue

$$P_l = \sum_{i=1}^{n_p} T_{li}\varepsilon_i \,, \quad \Rightarrow \quad \varepsilon_i = ?$$

where n_p is the number of pixels and
T_{li} is the element of the geometric matrix T

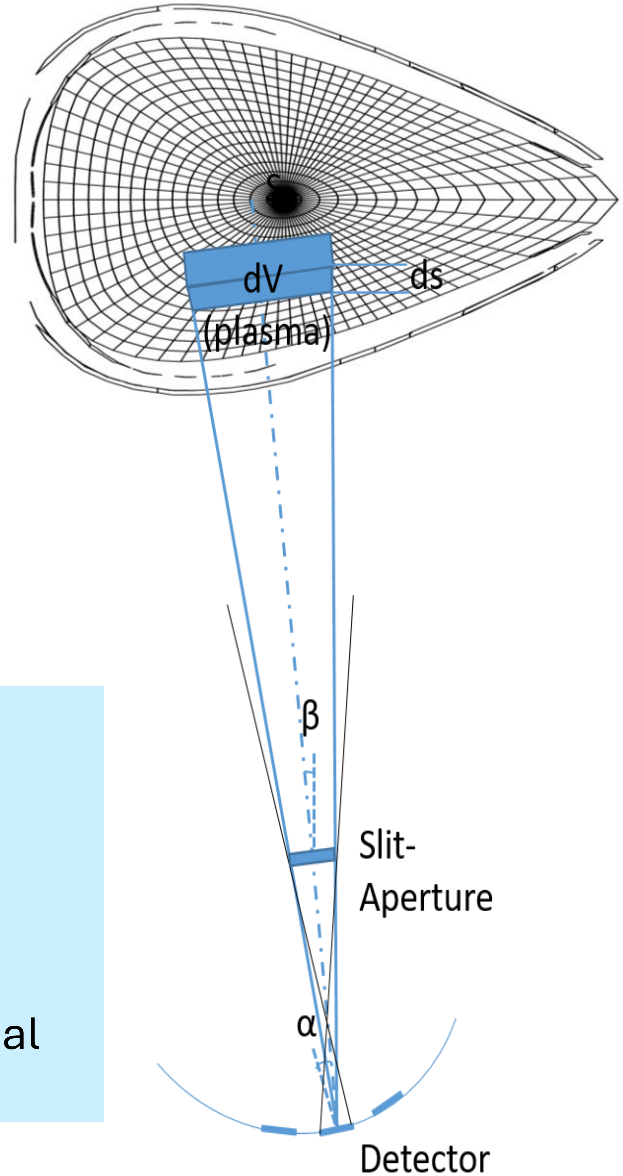

The challenges:

unknown parameters >> known conditions

(grids or pixel number~2000) (n_l = 65)

! under-determined, ill-posed problem.

!! Furthermore, the LoS of the bolometers has finite toroidal extension.

D. Zhang et al., Nucl. Fusion **61** (2021) 116043

A novel regularization functional invoking anisotropy: relative gradient smoothing (RGS)

- **The algorithm**

minimizing the function $\Phi = \frac{1}{2}\chi^2 + \lambda \cdot I_F$, where:

$$\chi^2 = \frac{1}{n_l}\sum_l \frac{\sum_i (T(i,l) * g(i) - P_l)^2}{\sigma(l)^2};$$

σ – error in l^th channel

➢ Minimum Fisher Regularization (MFR):

$$I_F = \int \frac{(g'(x))^2}{g(x)} dx$$

(Fisher information)

A smooth profile is obtained by optimizing λ until χ^2 ~1 is reached

[M. Anton et al., PPCF, **38** (1996) 1849]

- **Recent improvement**

using a novel regularization functional based on relative gradient smoothing function (RGS):

$$I_F = \int (\frac{g'(x)}{g(x)})^2 dx$$

⬇

$$I_F = \sum_{i=0}^{n_p-1} \frac{(k_r \nabla_r \varepsilon(i))^2 + (k_\theta \cdot \nabla_\theta \varepsilon(i))^2}{\varepsilon(i)^2}$$

➢ Implementing anisotropic smoothness factor $k_{ani} = k_\theta / k_r \sim 20 - 50$ [Fuchs, J., et al., EPS, 1994]

➢ Code validation using 3D modeling

[D. Zhang, H. Thomsen et al., 40th EPS (2013)]

Testing the tomography technique

- Using modelling results of oxygen radiation (EMC3-Eirene) as phantom
- Create synthetic data by multiplying by geometry matrix (forward model)
- Add 3% gaussian noise (similar to detector noise)
- Perform tomographic inversion
- Compare to phantom
- Use geometry matrix with inversion to calculate inversion brightness
- Compare with synthetic data from phantom shows goodness of reconstruction

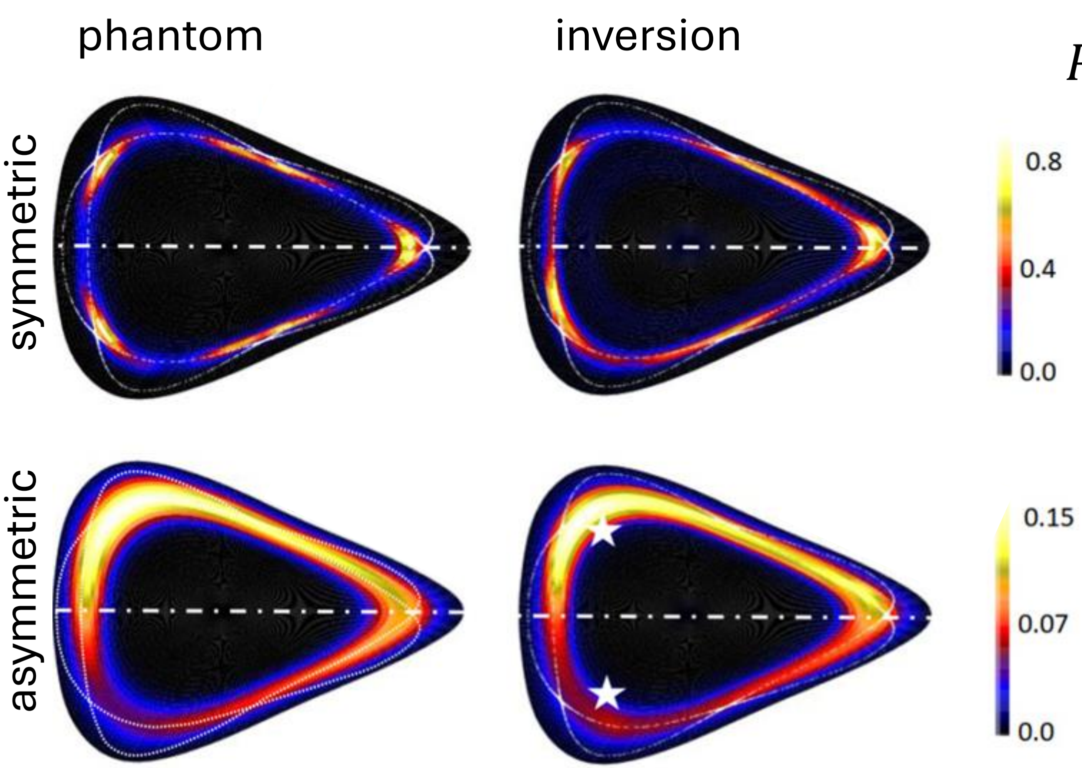

$$P_l = \sum_{i=1}^{n_p} T_{li}\varepsilon_i \,,$$

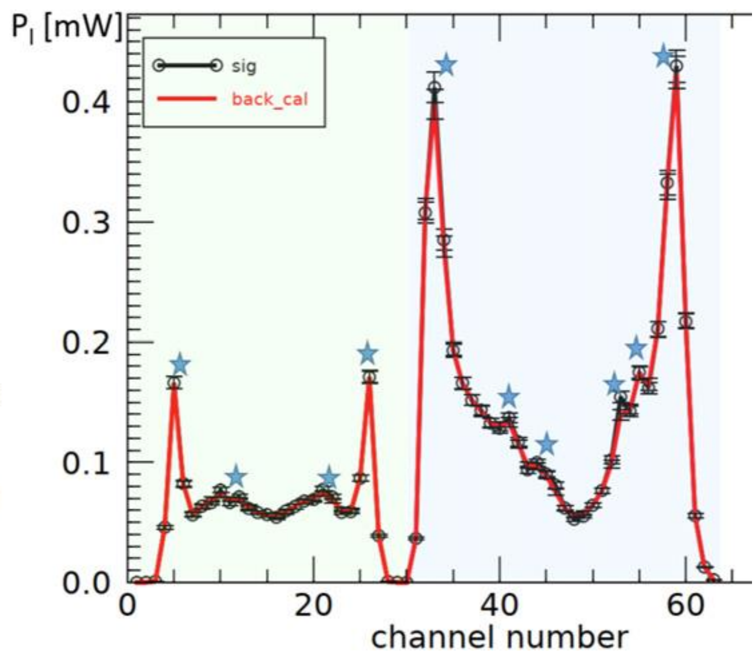

D. Zhang et al., Nucl. Fusion **61** (2021) 116043

Imaging Bolometer for ITER: Advantage of Toroidal View

Top view of ITER mid-plane

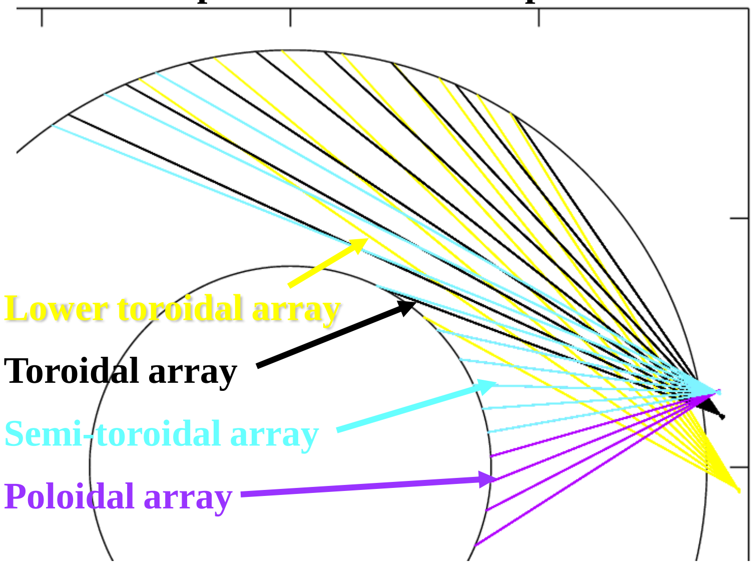

As arrays become more toroidal spatial and angular coverage improve

Poloidal projection of LOS:

Maps lines of sight (LOS) back to one poloidal cross-section to show spatial coverage assuming axi-symmetry

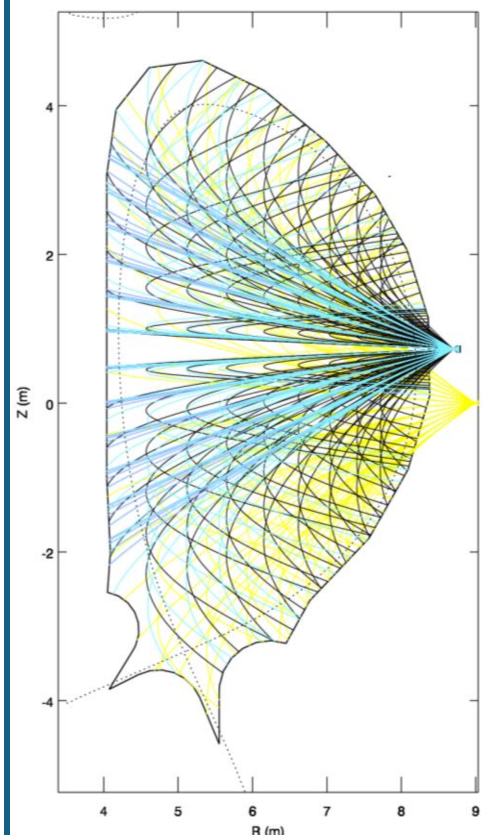

analysis tools developed by L.C. Ingesson

Imaging Bolometer for ITER: Advantage of Toroidal View

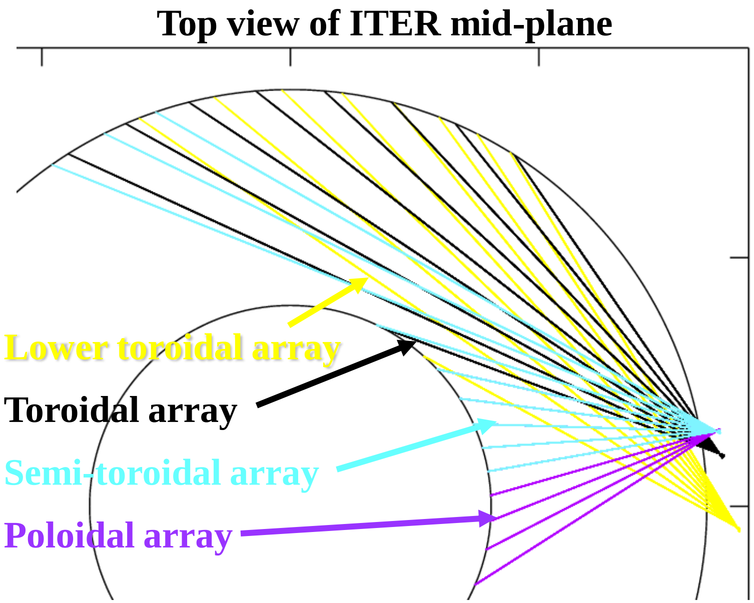

As arrays become more toroidal spatial and angular coverage improve

analysis tools developed by L.C. Ingesson

Poloidal projection of LOS:

Maps lines of sight (LOS) back to one poloidal cross-section to show spatial coverage assuming axi-symmetry

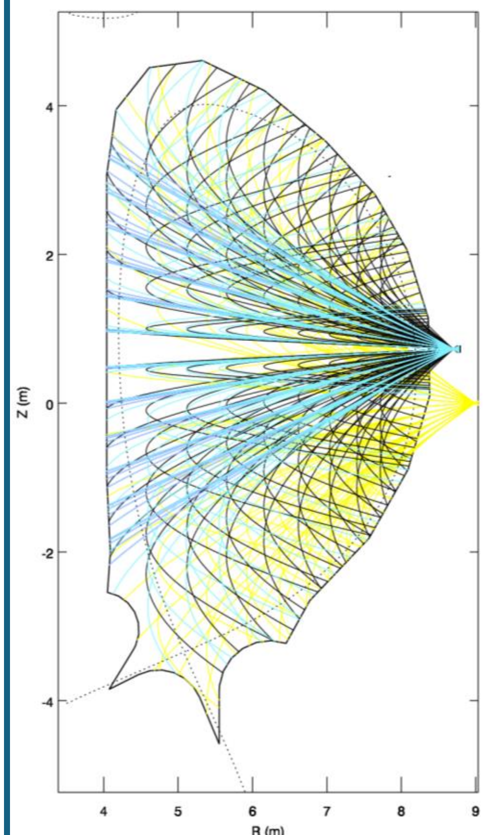

Compared with multiple resistive bolometer camera arrays at one poloidal cross-section

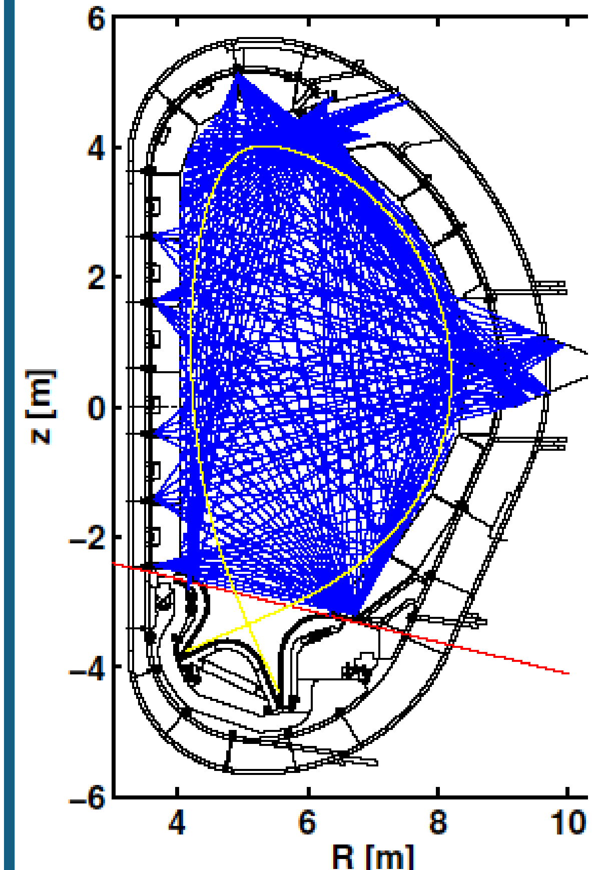

KSTAR IRVB with tangential view

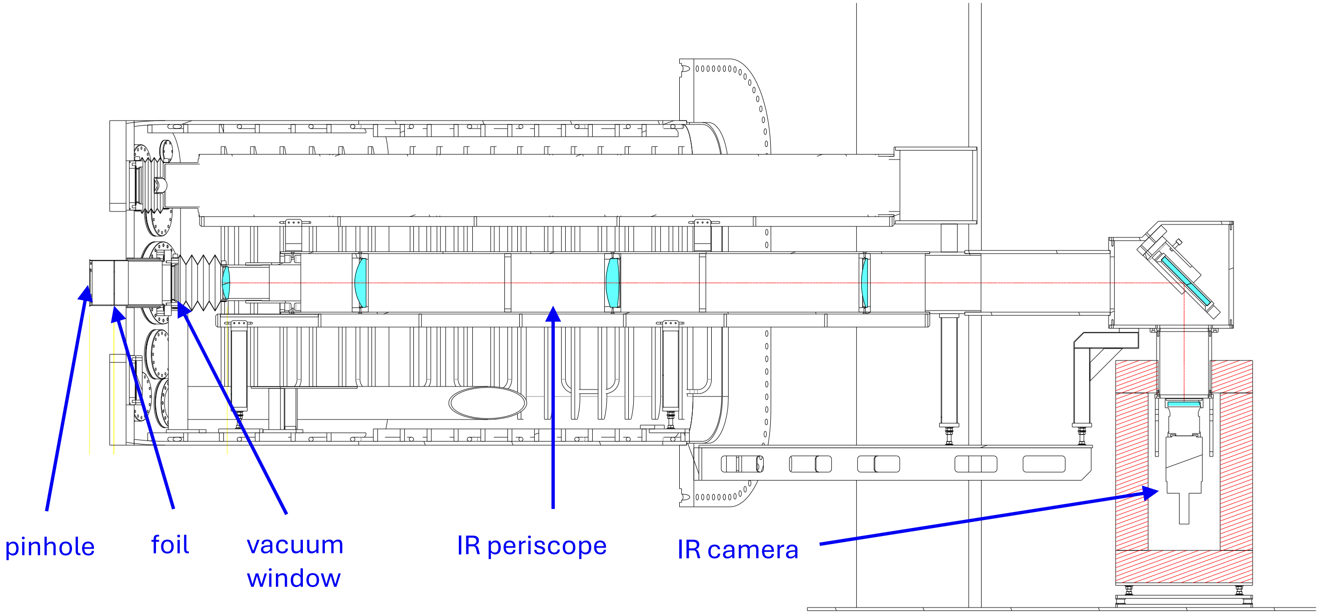

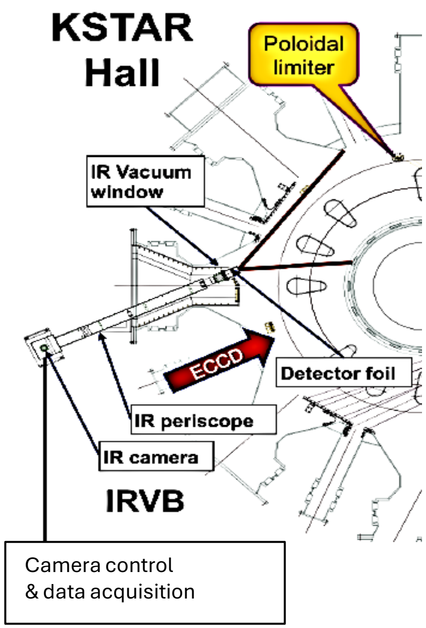

Aperture : 3.5 mm x 3.5 mm

Platinum foil

- ✓ Size : 0.002 x 70 x 90 mm
- ✓ Double side carbon coating

IRVB system

- ✓ Time resolution : 10 ms
- ✓ Photon energy range :
  E_{ph} < 7.5 keV
- ✓ 24(tor) x 32 (pol) = 384 ch

IR camera : FLIR SC7600

- ✓ Detector : InSb (Indium Antimonide)
- ✓ NETD : < 20mK
- ✓ Spectral range : 1.5 ~ 5.1 um
- ✓ Frame rate : 105 Hz
- ✓ Resolution : 512 x 640 pixels

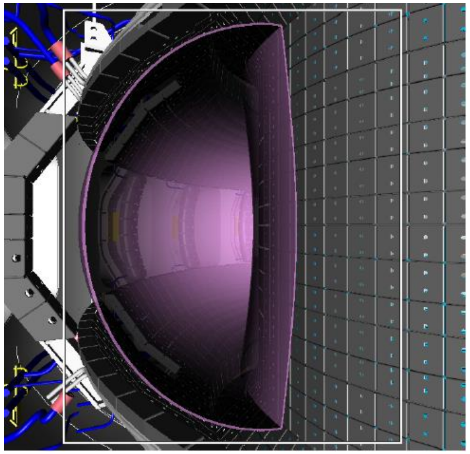

IRVB field of view

S.Oh, J-K diagnostics meeting (2019)

KAIST IERC

Tomography

A non-invasive imaging tool for observing the inner structure of the plasmas

Tangential line integration

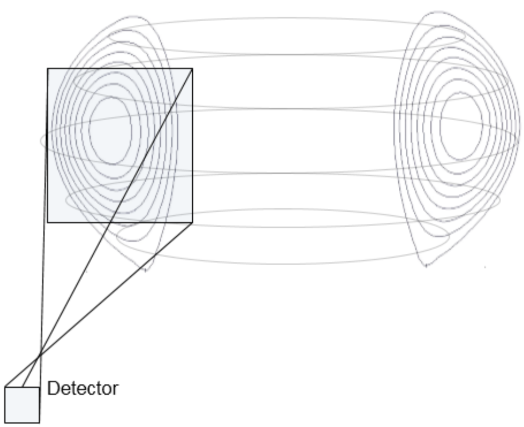

Ill-posed problem

$$\mathbf{f} = \mathbf{W} \cdot \mathbf{g}$$

f : Line-integrated image
W : Geometry matrix
g : Local emission profile (2-D)

Local emission profile
(poloidal cross-section)

↓

3-D geometry
(with toroidal symmetry)

↓

Line-integration

↓

IRVB image

Reconstruction

Phillips-Tikhonov method*

- Minimizing J = mean squared error + signal variation

$$J = |f - W \cdot g|^2/M + \gamma|L \cdot g|^2$$

- P-T solution ($\partial J/\partial g_i = 0$)

$$\mathbf{g}(\gamma) = \left(\mathbf{W}^{\mathbf{T}} \cdot \mathbf{W} + \mathbf{M}\gamma\mathbf{L}^{\mathbf{T}} \cdot \mathbf{L}\right)^{-1} \cdot \mathbf{W}^{\mathbf{T}} \cdot \mathbf{f}$$

g : Reconstructed image
γ : Optimal regularization parameter
L : Laplacian
M: number of detector channels

- **GCV statistics : optimized γ**
  → *accuracy vs smoothness*
  → high γ : smooth, inaccurate
  → low γ : accurate, unstable to noise

*S. H. Lee et al, Rev. Sci. Instrum. **83** 10E512 (2012)

Reconstruction grid

- 2 cm x 2 cm pixel was used for reconstruction test
- Reconstruction for pixels smaller than 1cm is ongoing for P_{SOL} calculation.
- Material boundary condition of KSTAR is applied to reconstruction code.

12x16 → 24x32 channels

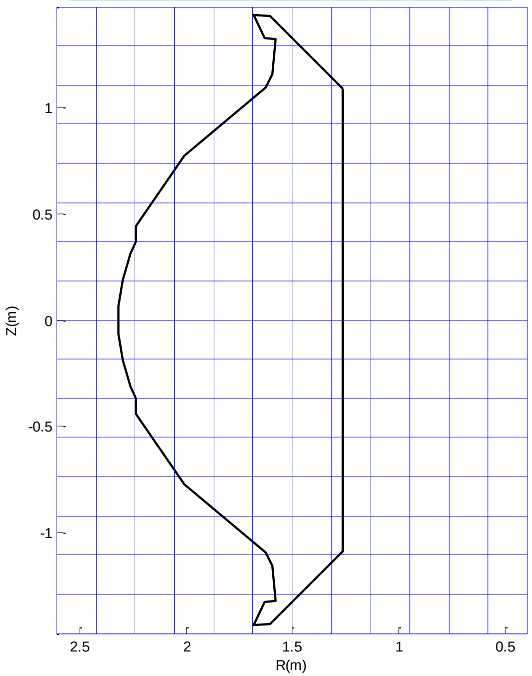

Bolometer view

1.27 < R < 2.52m,
-1.5 < Z < 1.5m

63x150 pixels
(~2x2 cm²/pixel)

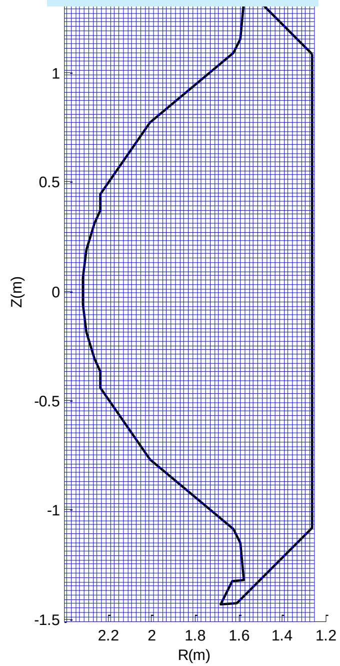

Reconstruction grid

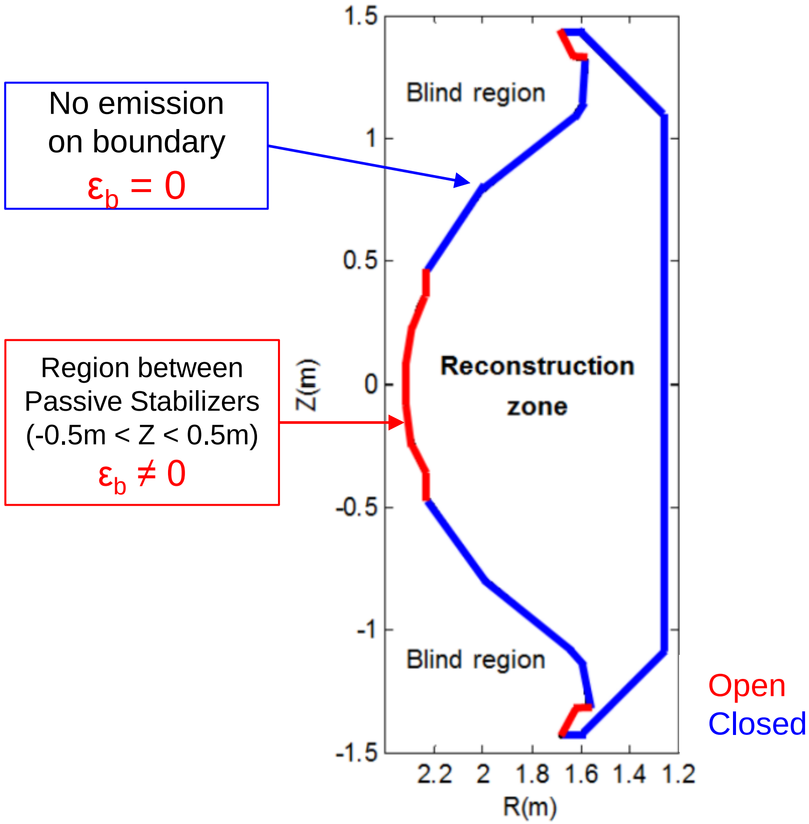

Boundary condition of divertor

Reconstruction of synthetic data from phantoms gives confidence in technique

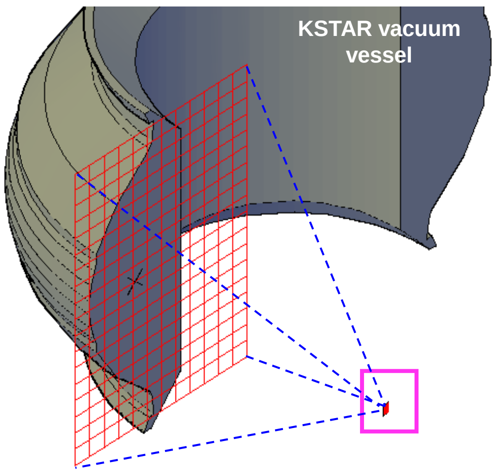

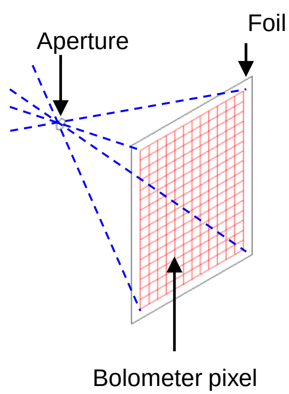

$$Ill-posed\ problem$$
$$\mathbf{f} = \mathbf{W} \cdot \mathbf{g}$$
$$f:\ Line-integrated\ image$$
$$W:\ Weight\ matrix$$
$$g:\ Local\ emission\ profile\ (2-D)$$

Phantom tests with D-shape and hot spots near divertor*

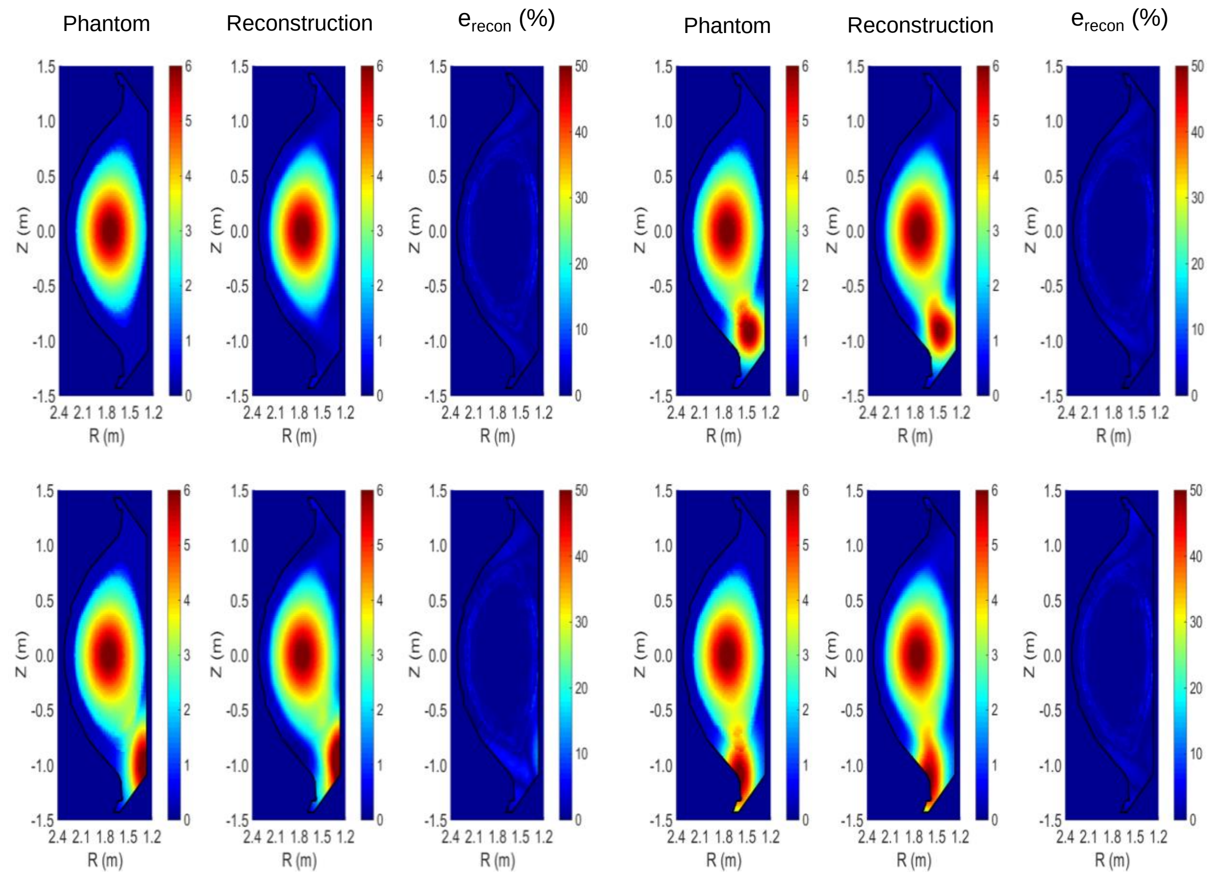

Tangential reconstruction code for KSTAR IRVB has been developed

- ✓ Phillips-Tikhonov method with toroidal symmetry assumption
  - → removing line integration effect
- ✓ **Accuracy of reconstruction was validated with phantom tests.**

Imaging bolometer is routinely providing all the radiated power information on KSTAR

- Post-shot 2D radiation profiles
  - using Phillips-Tikhonov algorithm
- total radiated power

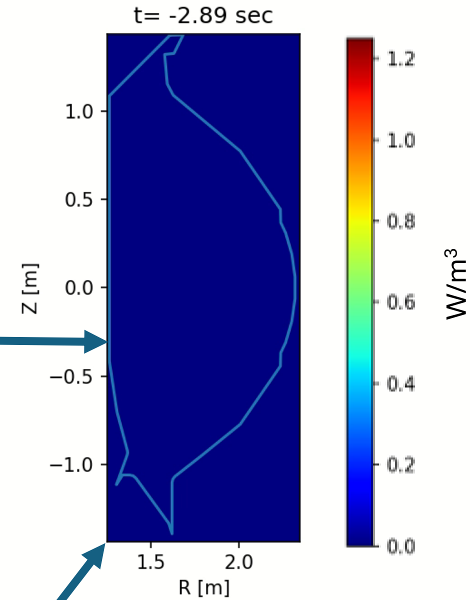

2D radiation profiles (100 x 100 voxels)

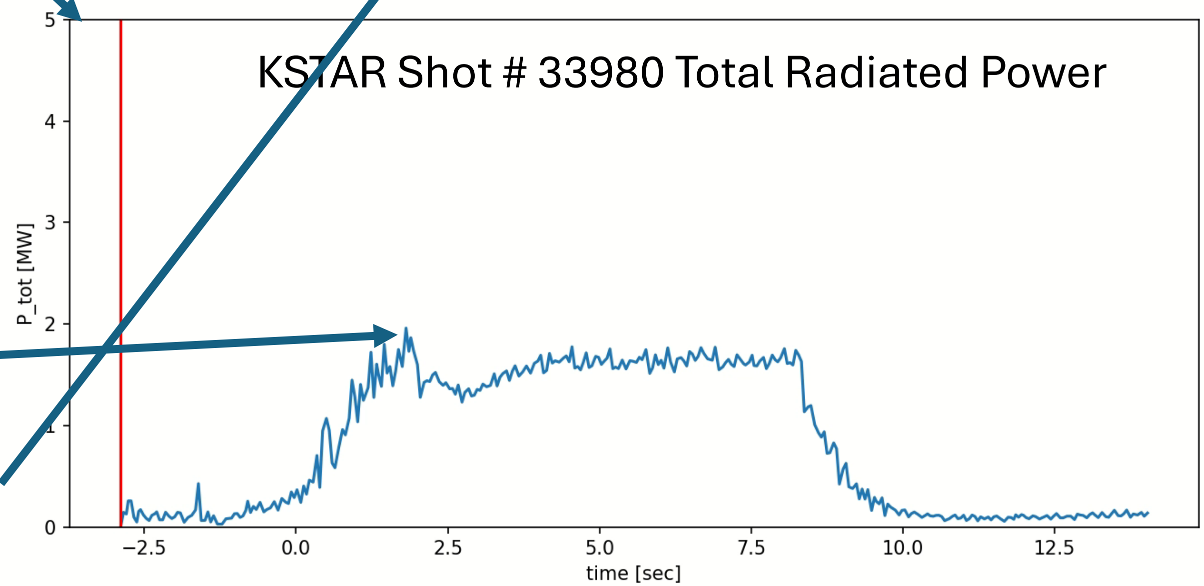

- W accumulation
- diagnosed by IRVB
  - with tangential view

Courtesy of S. T. Oh, KFE, Korea

3D tomography in LHD with 4 IRVBs

Total 3196 ch

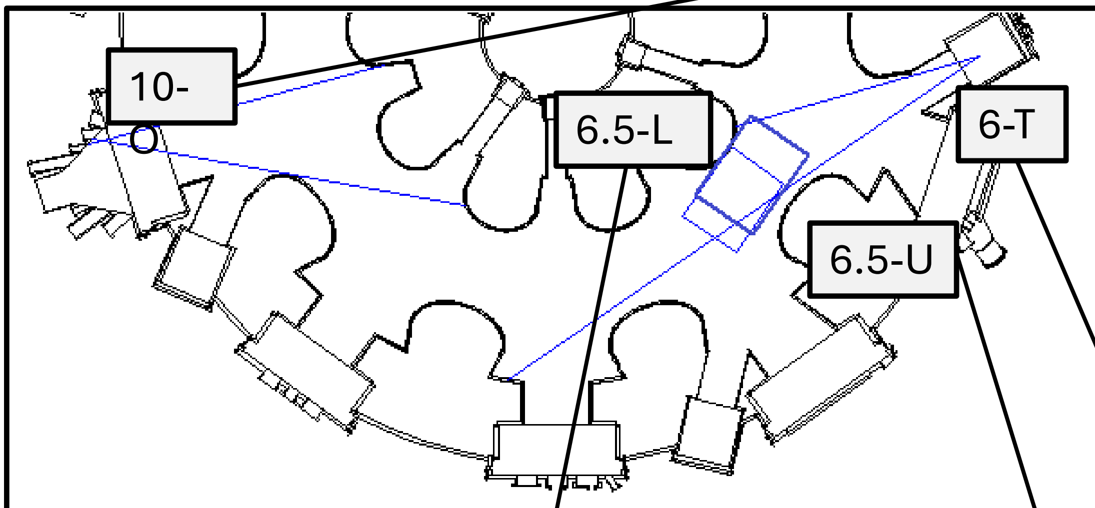

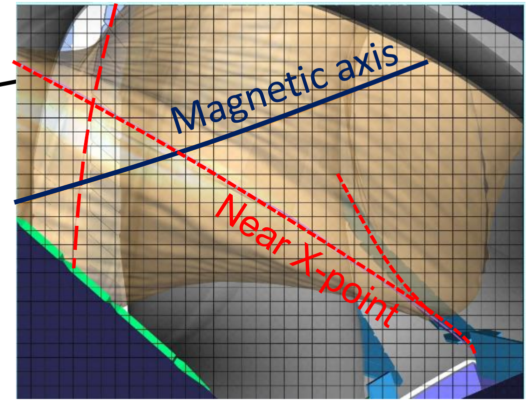

10-O IRVB (semi-tangential outer port)

36x28= 1008 ch

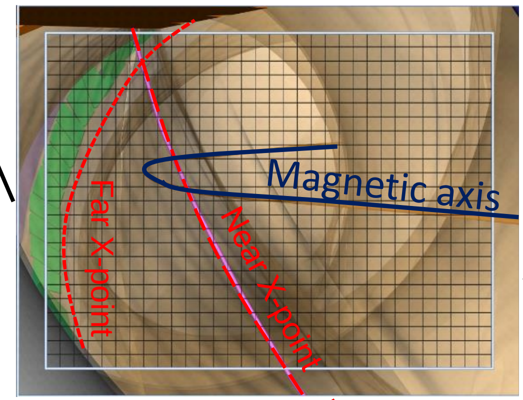

6-T IRVB (tangential port)

36x28= 1008 ch

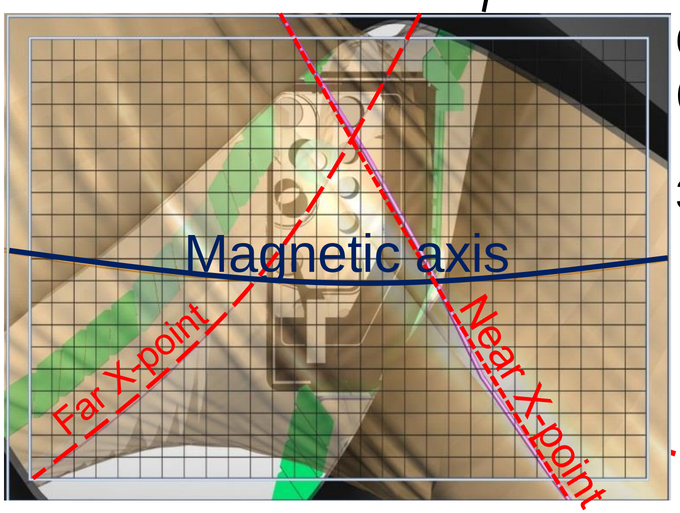

6.5-L IRVB (lower port)

30x22= 660 ch

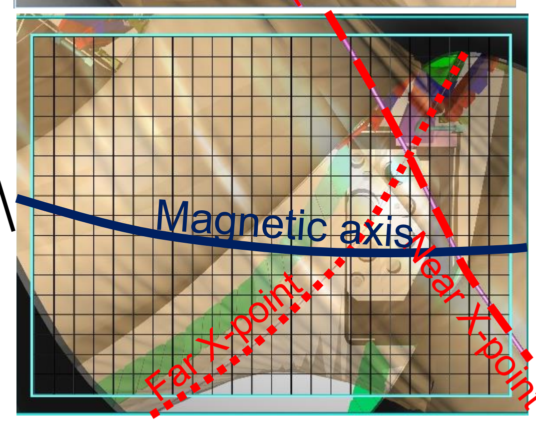

6.5-U IRVB (upper port)

26x20= 520 ch

SOKENDAI

Geometry matrix calculation for synthetic diagnostic for LHD IRVB

- Plasma is divided into volumes using R, z, ϕ
- ΔR = 5 cm, Δz = 5 cm, $\Delta\phi$ = 1 degree
- 2.5 m < R < 5.0 m (50 divisions)
- -1.3 m < z < 1.3 m (52 divisions)
- ϕ = 0 - 18 degrees (18 divisions) assume helical symmetry $S(R,\phi,Z) = S(R,36-\phi,-Z)$
- total 46,800 cells
- Intersection of plasma volumes and bolometer chord volumes, V_{ij}, is determined using subvoxels < 1 cm
- Solid angle, Ω_{ij} for the center of each subvoxel is calculated

$$\Omega_{i,j} = A_{\mathrm{det}} / d^2$$

- Write system of equations for detector power, P_i, and volume emissivity, S_j

$$P_i = \sum_j \frac{\Omega_{ij}}{4\pi} V_{ij} S_j = \sum_j T_{ij} S_j$$

- Then geometry matrix, T_{ij}, is determined
- 3-D C radiation data from EMC3-EIRENE is resampled to 5 cm x 5 cm x 1° is used as S_j to calculate P_i at detector
- Use code data to remove non-radiating voxels from edge (by factor 3) to 16,188 cells
- At each step location of subvoxels is checked to make sure it is within plasma subvolume region and does not intersect wall.
- avg 44 sightlines per voxel, maximum is 113
- all plasma voxels can be observed by at least one IRVB channel

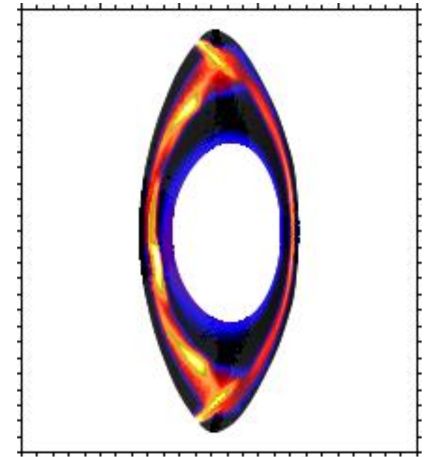

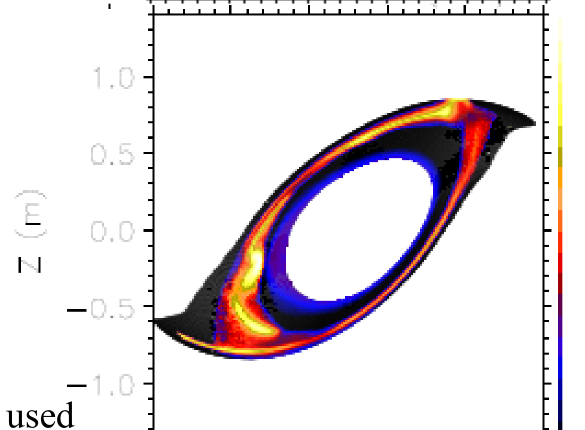

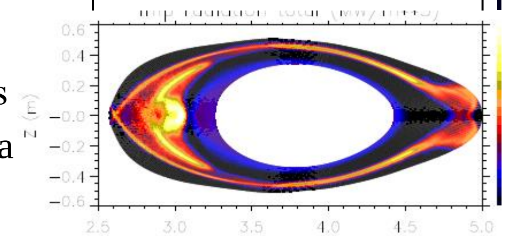

3D radiation profile related to IRVB images by geometry matrix

$\mathbf{P} = \mathrm{H}\mathbf{S}$

H:Projection matrix (Field of View) (3,196x16,188)
P: IRVB data(3,196 ch)
S:3D radiation profile (1 toroidal section) (16,188 voxels)

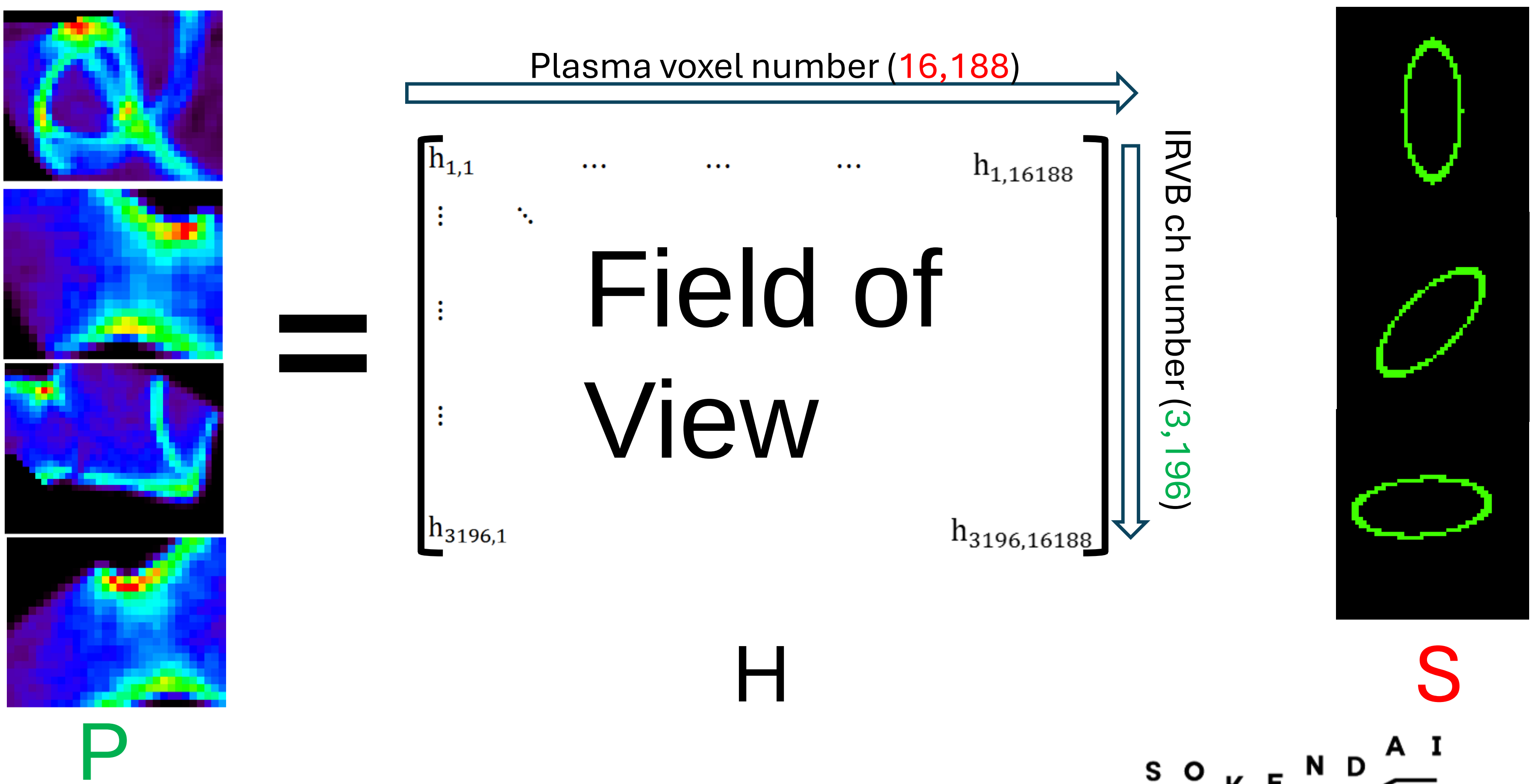

Tikhonov regularization for 3D plasma reconstruction

Lagrange function

$$\Lambda(\mathbf{S}) = \gamma\|\mathrm{I}\mathbf{S}\|^{2} + \frac{\|\mathrm{H}\mathbf{S}-\mathbf{P}\|^{2}}{\mathrm{M}}$$

H: Geometry matrix
P: IRVB data
S: 3D radiation profile
M: IRVB channel number
γ: Regularization parameter
I: Identity matrix

Series expansion with minimum Λ [2]

$$\hat{\mathbf{S}} = \sum_{j=1}^{M} w_j a_j I^{-1}\mathbf{v}_j$$

$$w_j = \frac{1}{1 + M\gamma/\sigma_j^2}$$

$$a_j = \frac{\langle \mathbf{u}_j \cdot \mathbf{P} \rangle}{\sigma_j}$$

j : index of IRVB channel
$\mathbf{v}_j$: j-th row vector of right singular matrix of HI^{-1}
$\mathbf{u}_j$: j-th row vector of left singular matrix of HI^{-1}
σ: j-th singular value

Reconstruction result is determined by **P** and γ.

[2]N. Iwama *et al.*, J. Plasma Fusion Res. **82** (7), 399 (2006)

3D tomographic inversion shows radiation region shrinks from inboard to outboard.

LHD #121787 Rax=3.9m

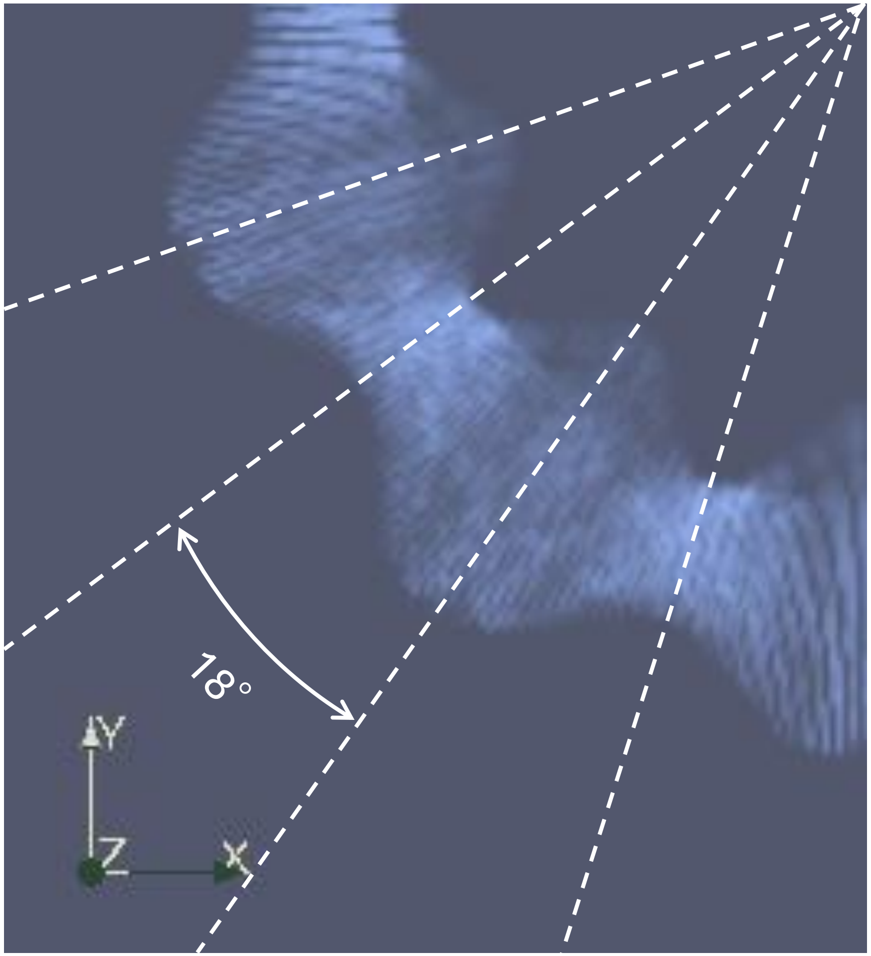

- Using a Tikhonov regularization
- Assume plasma repeats every half field period (18°)

- 3D tomography shows evolution of radiation region.
- Shrinking
- Inboard enhancement

MAST-U IRVB with tangential view of super-X divertor

- IRVB in MAST-U aimed at the lower x-point to complement the resistive bolometry system

- Poloidal view of MAST-U showing the comparison of the resistive bolometer system LOS (magenta) with a colour plot indicating the regions of higher sensitivity of the IRVB.

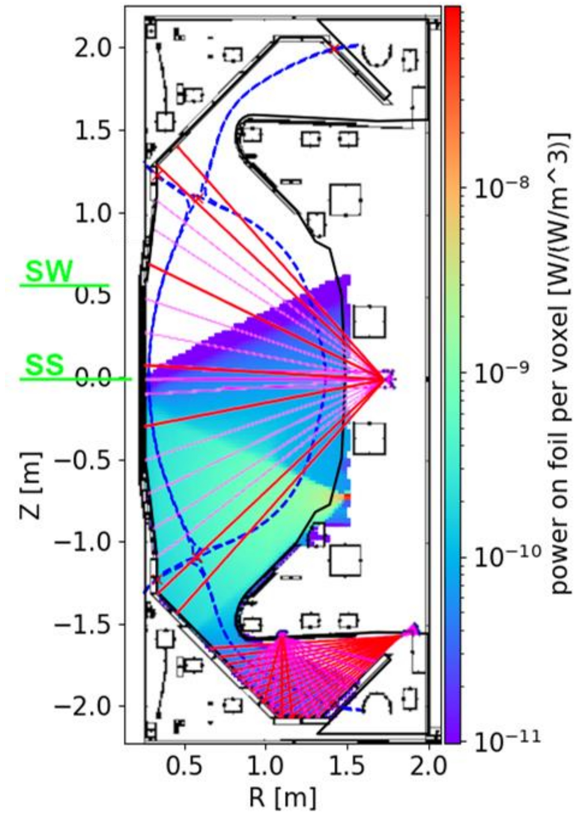

IRVB Design:
- $D_{aperture}$ = 4 mm
- $L_{f\text{-}ap}$ = 45 – 60 mm
- Foil: Pt 2.5 μm x 9 m x 7 cm, coated with 10 μm graphite
- IR camera: FLIR SC7500 (383 fps, ~45k pixels)
- IRVB: ~3900 channels, 192 fps, NEPD = ~0.8 W/m^2

- Top view of MAST-U showing the position of NBIs (green), of the co- and counter-NBI resistive bolometer LOSs and the IRVB FOV (yellow, mostly counter-NBI).

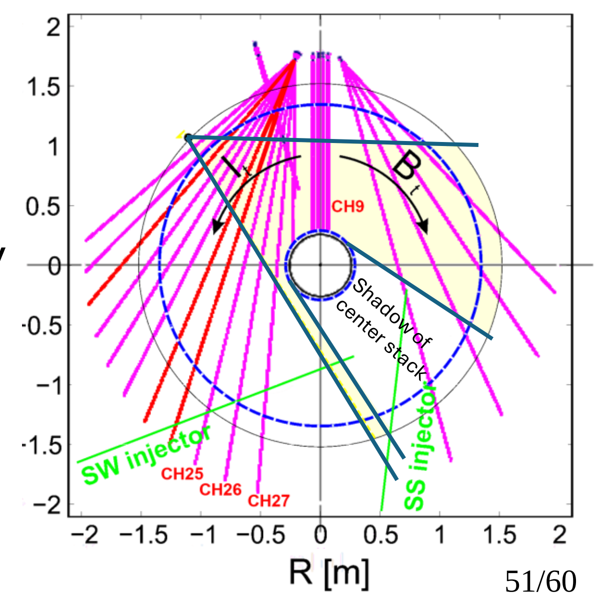

CCFE CULHAM CENTRE FOR FUSION ENERGY

UNIVERSITY of York

Tomographic inversion

Once the geometry and area of the foil is defined a method to perform the inversion can actually be devised

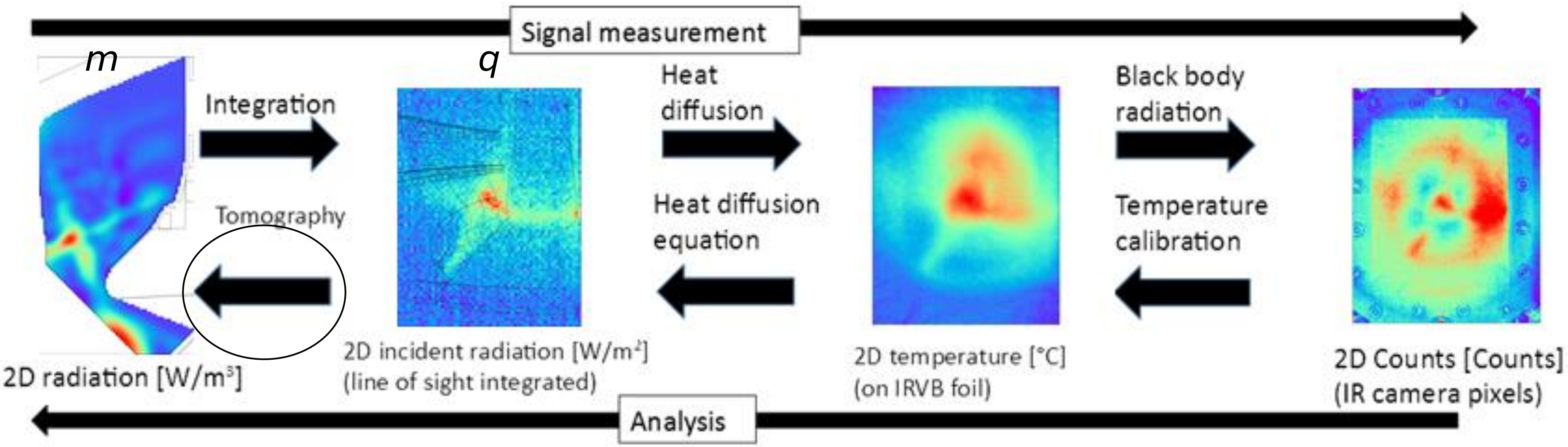

Ideally:

$$r = ||\boldsymbol{W}m - q|| = 0$$

with

$\boldsymbol{W}$ = geometry matrix

r = residuals

m = real emissivity solution

q = theoretical brightness measurement

With real data solving for q would return an exact solution, but dominated by noise

SART with Phillips-Tikhonov Regularization

- Simultaneous Algebraic Reconstruction Technique (SART)
  - Iterative technique to find solution *m'*
- penalty function ***L***
  - weight given to each spatial pixel in relation to each other and
- regularization coefficient α
  - introduced to limit the irregularity of the solution:

$$||\boldsymbol{W}m' - q|| + \alpha^2||\boldsymbol{L}m'||$$

- This is ≠ 0 and it is minimized to find the solution.
- Different types of penalty functions depending on what type of regularity is desired *on the emissivity solution*

First derivative

	-1	
-1		1
	1	

Partial second derivative

	-1	
-1	4	-1
	-1	

Full second derivative

-0.5	-1	-0.5
-1	6	-1
-0.5	-1	-0.5

Simplified second derivative

-1	-1	-1
-1	8	-1
-1	-1	-1

most common

- How to determine the optimal parameter α?
  - Perform a scan in α
- Balance regularity with the most information on the real profile conserved:
  - α at which the L-curve has the highest curvature

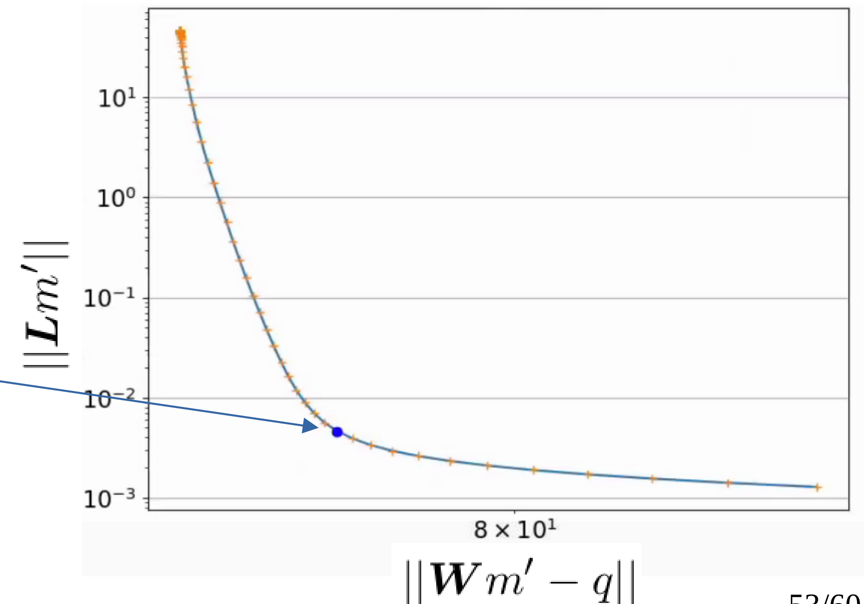

CCFE CULHAM CENTRE FOR FUSION ENERGY

UNIVERSITY of York

Bayesian approach considers other factors

Bayesian approach:

Signal noise: The measured camera data is evaluated based on its uncertainty (σ_k).

$$||\boldsymbol{W}m' - q|| \longrightarrow -\frac{1}{2}\sum_{k=1}^{m}\left(\frac{q_k - \hat{q}_k}{\sigma_k}\right)^2$$

Forward modelled term $$\hat{q}_k = \sum_{l=1}^{n} W_{k,l} m'_l$$

Negative emissivities: Negative weight to penalize negative emissivities can be added

$$-(200)^2 \sum_{l=1}^{n}\left(\frac{\min(0, m'_l)}{10^6 W/m^3}\right)^2$$

CCFE CULHAM CENTRE FOR FUSION ENERGY

UNIVERSITY of York

Considering Resistive Bolometer Signals

Bayesian approach:

Further measurements/factors can be included to increase confidence:

Resistive bolometer data: Solution *m'* → brightness as measured from resistive bolometry lines of sight (r)

Penalty added to the function to be minimized

$$-\frac{1}{2}\sum_{r}\frac{R_{r,l}m'_{l}-q_{r}}{\sigma_{r}}$$

R = geometry matrix of the resistive Bolometry system

σ_r = uncertainty of the resistive bolometry measurement

Also:

Uncertainties in IRVB geometry and foil properties

Field of view of MASTU IRVB (color) compared to the resistive bolometry lines of sight (lines)

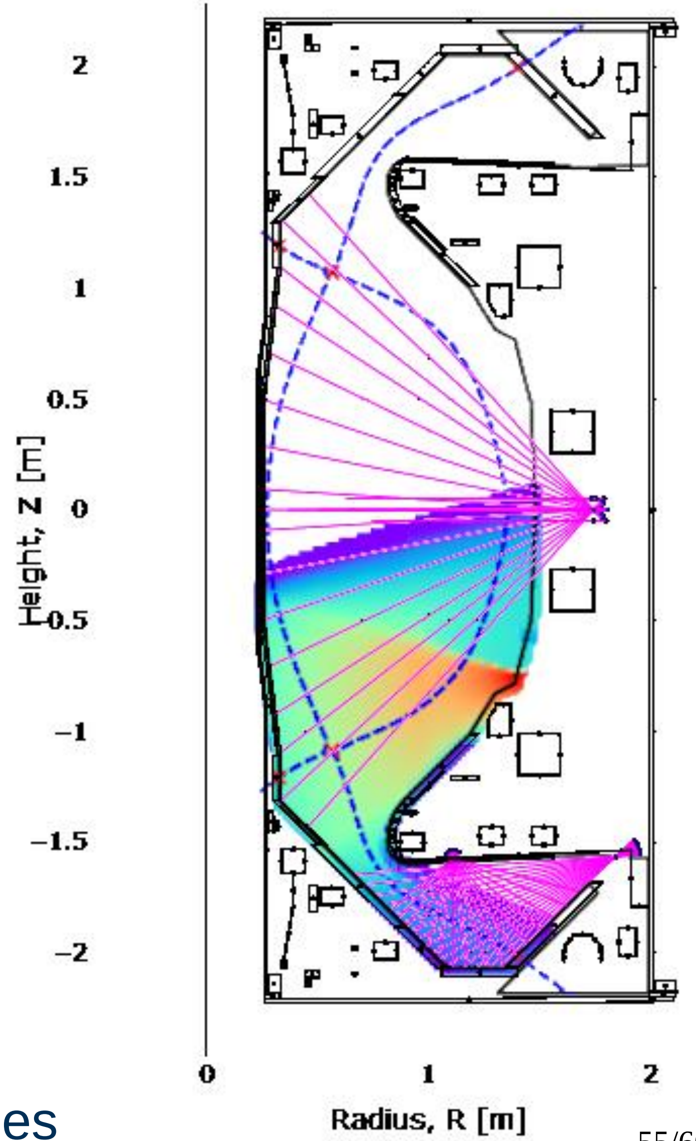

Spurious IRVB signal sources considered

Further corrections:

Contribution to foil brightness due to the pinhole plate heating

$$\hat{q}_k = \sum_{l=1}^{n} W_{k,l} m'_l \longrightarrow \hat{q}_k = \sum_{l=1}^{n} W_{k,l} m'_l + Q_k$$

Aperture plate heated by the plasma radiation and reradiates heating foil

Black body radiation due to the pinhole plate heating modelled based on Tmin, Tmax, and the slope of the temperature curve

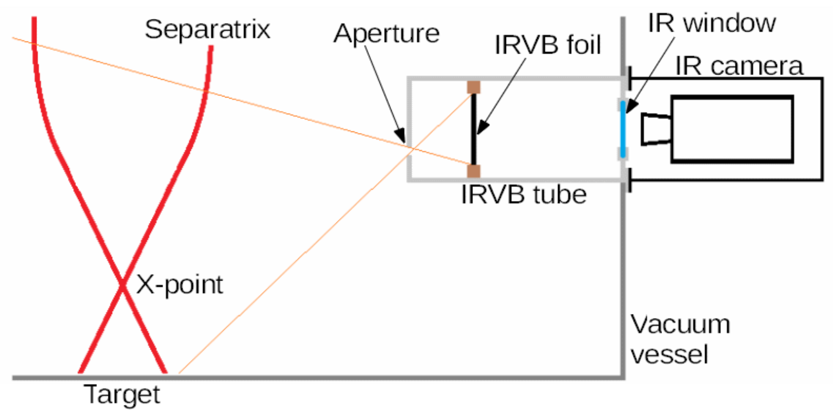

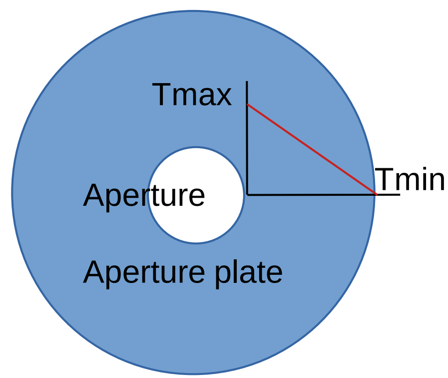

Comparison using self-generated phantom

T-P SART | Phantom | Bayesian

Non field aligned feature, unphysical

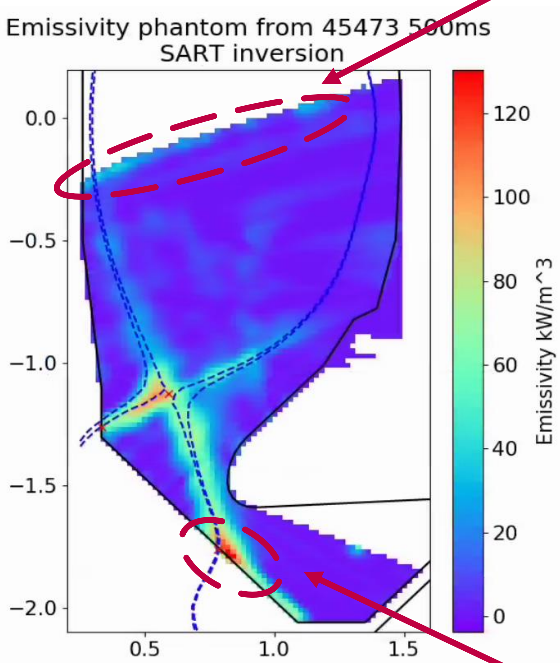

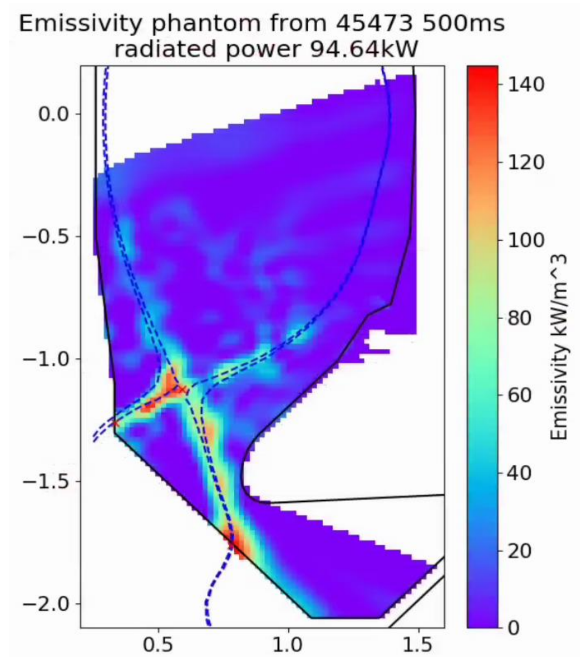

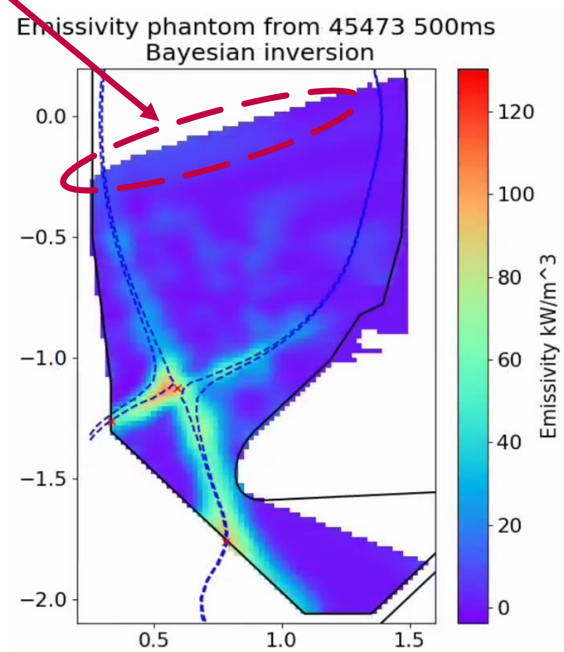

More peaked emission (likely a positive)

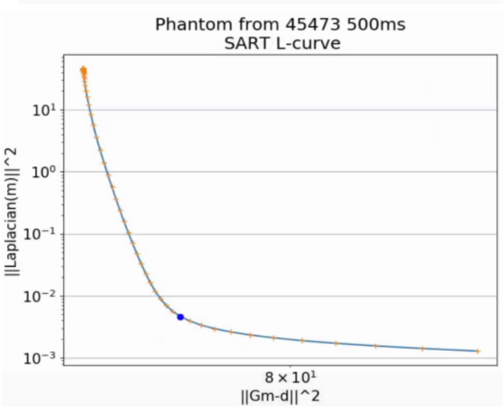

Comparison between SART/Bayes results and the input phantom	SART	BAYES
Radiation std all volume [W/m³]	675.7	700.72
Radiation std below x-point [W/m³]	972.86	1059.00
Total radiated power variation [%]	-11.18	-13.95
Total radiated power variation below x-point [%]	-11.09	-12.65
Total radiated power variation within 10cm of x-point [%]	-15.27	-15.47

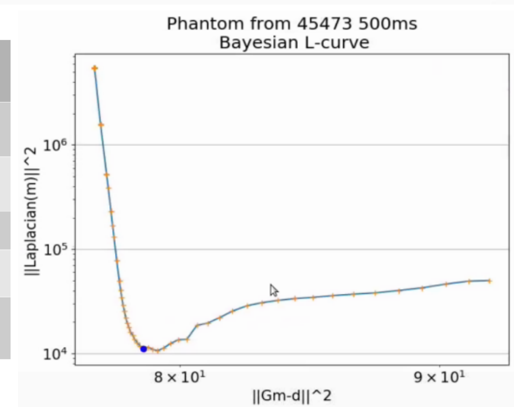

Comparison using real data

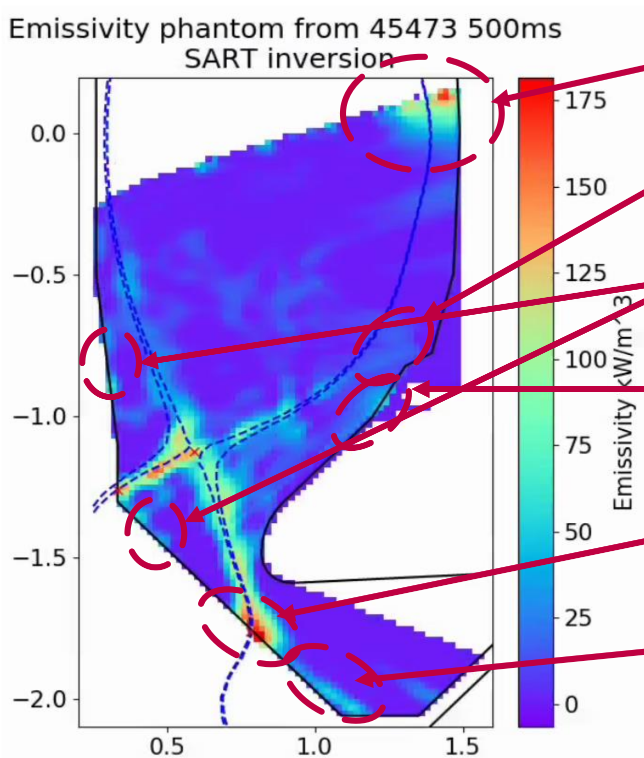

- Non field aligned artifacts, unphysical
- High emissivity stripes aligned to the pinhole LOS
- High emissivity close to surfaces far from separatrix, unphysical
- Strong brightness as close as possible to the pinhole (compensates for offsetts)
- More peaked emission (likely a positive)
- Radiated power elongated in the super-x chamber

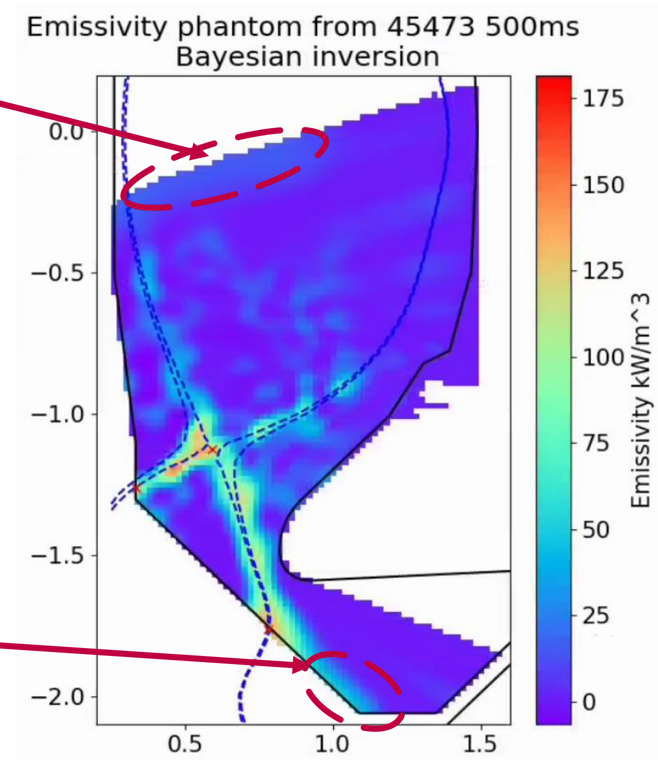

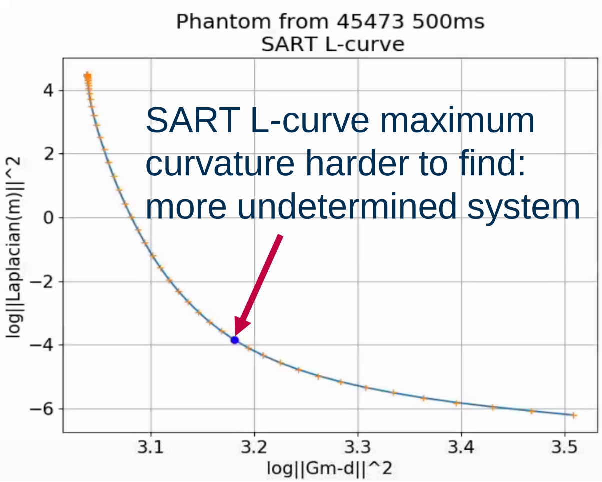

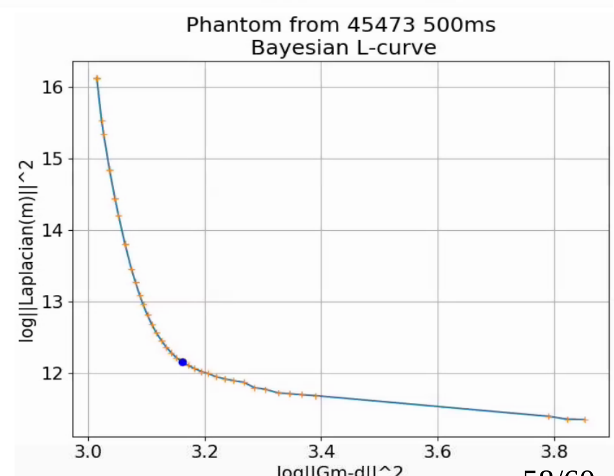

Conclusions

- Bolometers measure total radiated power from plasma
  - Resistive bolometers used in 1D arrays for 1D or 2D tomography at one toroidal angle
  - Imaging bolometers can provide thousands of channels
    - with a 2D (toroidal and poloidal) view of plasma
    - In a tokamak (axisymmetry) with tangential view enables 2D tomography
- Geometry matrix links local and FoV integrated information and used for:
  - Synthetic instrument
    - Direct comparison with line-integrated data
    - Diagnostic design
  - Tomography
- Tomography
  - Used for converting line-integrated data to local information in 1, 2, 3-D
    - you define the plasma grid depending on assumptions and detector type and number
  - Regularization is used in under-determined problems to make trade off between information and stability
  - Different schemes can be used to consider:
    - Anisotropy in radiation profiles with poloidal asymmetry (RGS in a stellarator)
    - Spurious signals, other diagnostics, detector noise, negative values, etc. (Bayesian)

Conclusions

- Bolometers measure total radiated power from plasma
  - Resistive bolometers used in 1D arrays for 1D or 2D tomography at one toroidal angle
  - Imaging bolometers can provide thousands of channels
    - with a 2D (toroidal and poloidal) view of plasma
    - In a tokamak (axisymmetry) with tangential view gives 2D tomography
- Geometry matrix links local and FoV integrated information and used for:
  - Synthetic instrument
    - Direct comparison with line-integrated data
    - Diagnostic design
  - Tomography
- Tomography
  - Used for converting line-integrated data to local information in 1, 2, 3-D
    - you define the plasma grid depending on assumptions and detector type and number
  - Regularization is used in under-determined problems to make trade off between information and stability
  - Different schemes can be used to consider:
    - Anisotropy in radiation profiles with poloidal asymmetry (RGS in a stellarator)
    - Spurious signals, other diagnostics, detector noise, negative values, etc. (Bayesian)

Please see lecture on Friday by Dr. Rainer Fischer on Bayesian Inference!